VUV and X-Ray Free Electron Lasers:

The Technology and Its Scientific Promise

William Barletta and Carlo Rizzuto

Sections I & III – Motivations & FEL Physics

List of symbols

fine structure constant	α
dimensionless vector potential	a_w
horizontal Twiss α	α_x
bunching parameter	b
mean resolution error of BPMs	BPM_{res}
position error of BPMs	BPM_{pos}
remanent field	B_R
undulator magnetic field strength	B_w
horizontal Twiss β	β_x
speed of light	c
mean phase error in undulator	$\Delta\phi$
penetration depth	δ_p
horizontal dispersion	D_x
derivative of D_x	D'_x
FEL beam diameter on optic	D_w
energy chirp from CSR	$\delta E/E$
beam emittance	ε
electron charge	e
beam energy	E
peak electric field in gun	E_o
normalized emittance	ε_n
energy in the FEL pulse	E_{Pulse}
longitudinal space charge force	F_{sc}
angle of incidence	j_i

relativistic factor ($E/ m_e c^2$)	γ
optical function in transport	H
magnetic coercivity	H_C
Alfven current at γ=1	I_{Ao}
beam current	I_b
BBU threshold current	I_{BBU}
undulator parameter	K
mean undulator strength	K_{rms}
undulator spatial frequency	k_w
gain length	L_G
m^{th} harmonic wavelength	λ_m
plasma wavelength	λ_P
radiation wavelength	λ_r
undulator wavelength	λ_w
root of gain equation	μ
harmonic number	m
electron mass	m_e
number of electrons	N_e
electron density	n_e
number of undulator periods	N_u
radiation power	P
input laser power	P_{laser}
noise power	P_n
pole roll angle error	ψ
BNP (or Pierce) parameter	ρ
quantum FEL parameter	ρ'
atom density	ρ_A
quality factor	Q
dipole quality factor	Q_{dipole}
FEL energy constraint ratio	r_1
FEL emittance constraint ratio	r_2
FEL diffraction constraint ratio	r_3
classical radius of electron	r_e
bend angle in undulator	θ
bend angle in achromat	Θ

phase of i^{th} electron	θ_i
kick relative to each pole error	ϑ_j
mean energy spread of electrons	σ_e
bunch length	σ_z
relativistic plasma frequency	ω_p
distance along undulator	z
mean longitudinal velocity	$<v_z>$
impedance of free space	Z_o
Rayleigh range	Z_R

I. Introduction: Why Free Electron Lasers?

I.A. Motivations

Chemical, physical, and biological processes are intrinsically dynamic in nature since they are related to electronic and atomic structures that evolve with time. The characteristic time scales span from a few femtoseconds, in the case of electronic processes, to a few tens or hundreds of femtoseconds, as in the case of atomic and molecular processes. Other phenomena, which control the behavior of critical systems, may happen at relatively longer time scales, ranging from a few picoseconds to a few hundreds of picoseconds or more. These phenomena include the dynamics produced in phase transitions, such as those related to magnetic order or to superconductivity. The nascent capability to measure these phenomena at the relevant time scales will open completely new perspectives and analyses. In particular, the direct observation of electronic processes, of structural dynamics and of dynamical critical phenomena (such as phase transitions) represents an unexplored landscape in the study of condensed matter. These possibilities were already evident to the inventors of the first coherent sources of femtosecond optical pulses. Ultra-short pulses of coherent light have generated remarkable scientific progress such as that which was recognized in the 1999 the Nobel Prize for Chemistry awarded to Ahmed Bewail for his pioneering work on the application of ultra-short laser infrared spectroscopy to the study of the dynamics of chemical bonds.

Currently available, fully coherent (laser) light sources emit radiation only in a limited range of wavelengths. Their use is limited to optical and spectroscopic techniques in the infrared, visible and near-ultraviolet range, excluding all the measurements needing photons of energy higher than a few eV. There is therefore a strong scientific need for a tunable, coherent light source with an energy range from the vacuum ultraviolet (VUV) to the X-ray with a stable and well-characterized temporal structure in the femtosecond and picosecond time domain. To this end, international research efforts are moving in three main directions: 1) laser-driven light sources which use non-linear processes to create very high harmonics, 2) interaction between an ultra-short laser pulse and an electron bunch in an storage ring (laser “bunch-slicing technique”), 3) free electron lasers (FELs). The first two techniques are able to produce radiation pulses in the femtosecond time domain and in the soft X-ray region with a relatively low brilliance (i.e. a low useful photon flux on the material under investigation). In contrast FELs can produce light pulses with peak brilliance as much as ten orders of magnitude higher than the pulses generated in present third generation synchrotron light sources and with photon energies ranging from the VUV to the hard X-ray, i.e. from about 10 eV (120 nm) to 10 keV (0.12 nm).

The performance of synchrotron radiation sources are commonly characterized and compared in graphs of the time-averaged flux (photons/s/mrad/0.1%BW) and brightness (photons/mm^2/mrad^2/0.1%BW) available for experiments as a function of X-ray energy. More recently other metrics have been proposed such as the useful flux within the phase space acceptance of a sample as small as a 50-100 micron protein crystal with a mosaicity of several milliradians. With increasing scientific interest in sub-picosecond pulses, the peak (or instantaneous) values of these metrics during a single pulse also

become important. Figure 1[1] compares the performance of several types of X-ray sources from the point of view of peak brightness and pulse duration. A listing of operating FEL facilities can be found on the internet at http://sbfel3.ucsb.edu/www/fel_table.html.

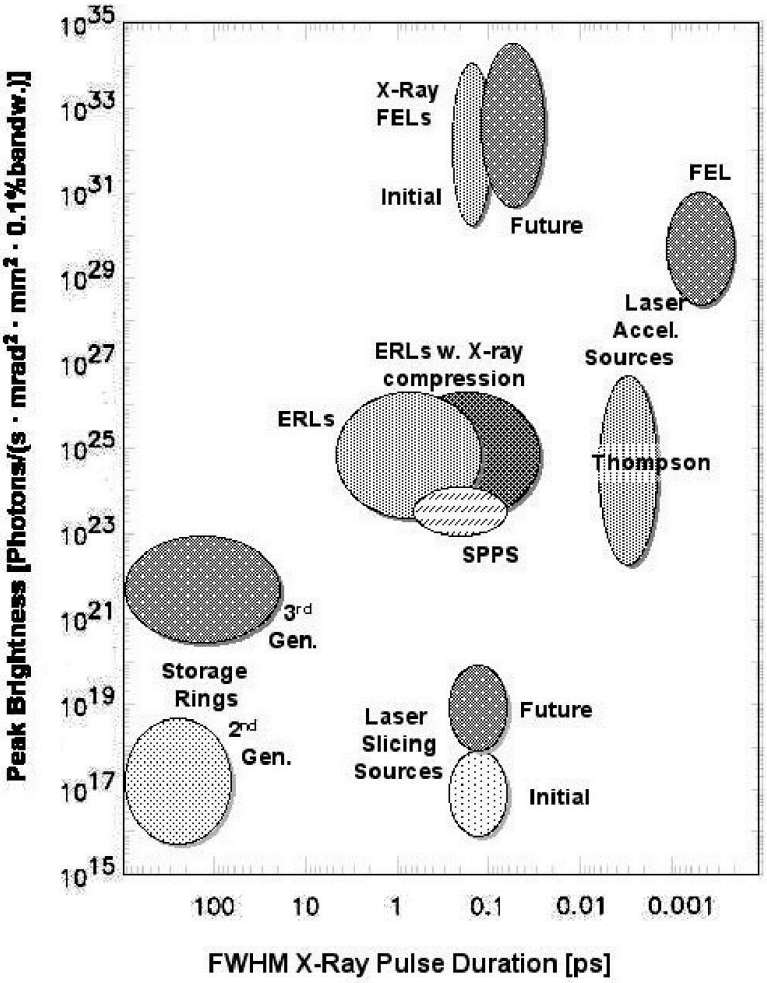

Figure 1. Brightness and pulse duration ranges of next generation light sources. The time average brightness is the peak brightness times the duty factor.

Table 1. Additional characteristics of UV/X-ray sources

	Maximum Duty Factor	Laser synchronization	Pulse repetition rate
Storage rings	~10^{-3}	No	10 – 100 MHz
Slicing Sources	~10^{-9}	Limited	1 – 10 kHz
Energy Recovery Linacs	~10^{-3}	No	10 – 100 MHz
ERLs w. X-ray compression	~10^{-8}	Yes	10 kHz
SPPS	~10^{-11}	No	100 Hz
X-ray FELs	~10^{-10}	Some	100 – 1000 Hz
Laser Accel. Sources	~10^{-12}	Yes	1 – 10 kHz

[1] Both the figure and table are reproduced from W. A. Barletta and H. Winick, "Introduction to special section on future light sources," Nucl. Inst. and Meth., A **500**, (March 2003) 1 – 10.

The performance metrics of Table 1[2] are likely to be used increasingly to complement the flux and brightness spectral curves that are already in general use, to assess the suitability of source performance for experiments that depend on the peak or instantaneous values.

The prospects for the blossoming of a new field of ultra-fast UV/X-ray science based on light produced by FELs (4th generation sources) in physics, chemistry and biology based on light produced by FELs (4th generation sources) are indeed exciting. Taking a lesson from the previous development of ring-based 3rd generation light sources, one anticipates that the real applications of FEL light sources will far surpass what is now predicted in the perspective scientific cases. Nonetheless, such research is likely to remain a relatively small part of the experiments that rely on storage ring-based synchrotron radiation sources. Storage rings sources are now, and are highly likely to remain, the workhorses of synchrotron radiation science for many years to come. By providing beams of radiation over a broad spectrum from the sub-mm radiation to X-rays with high flux and brightness and outstanding stability, reproducibility and reliability, storage rings sources will continue to serve the needs of a vast and still increasing scientific and technical community even while linac-based sources open up new scientific frontiers with their sub-picosecond pulse duration and extremely high peak brightness and coherence.

I.B. What users want in a FEL-based light source

As a most general performance metric of next generation light sources based on FELs and energy recovery linacs, users desire to have $\geq 10^{14}$ photons/sec in a 0.1% bandwidth delivered onto the experimental sample with a time structure matched to the physical process under investigation. This requirement can be expanded into requirements on spectral properties, bandwidth, tunability, pulse intensity, pulse duration, pulse-to-pulse stability, timing and synchronization, polarization, and repetition rate as described below.

Spectral properties

Processes of interest for investigation with FEL sources cover a large range of wavelengths from10 eV (120 nm) to 10 keV (0.12 nm). Some experimentalists are likely to want the same degree (or more) of spectral stability without monochromatization as is presently available from storage ring sources with monochromators.

Bandwidth

Not surprisingly, users request minimum spectral bandwidth and/or controlled chirp: bandwidth at the transform limit allows the user to isolate spectral shifts; spectral chirp allows correlating energy with time in new ways. For experiments measuring core level shifts 0.1-0.5 eV bandwidths are typical; for NEXAFS experiments a bandwidth of ≤ 0.1 eV is highly desirable. The most demanding requirement are for measurements of resonant inelastic X-ray scattering (RIXS) which calls for ultra-high resolution, $\Delta\lambda/\lambda \sim 10^{-5}$.

Tunability

Spectroscopy demands tuning near to edge transitions. Typically rapid tuning should be possible at the level of the spectral bandwidth. Tuning over tens of eV should be possible on the time scale of minutes.

[2] Id.

Pulse intensity

Even in the investigations of linear phenomena pulse intensities must be sufficient to obtain measurable photoemission signals and to record absorption contrast changes, without sample damage. The field intensities of the X-ray pulse must also be sufficient low to avoid Stark shift and field broadening of sample line widths. Typically such experiments in the linear regime cannot tolerate pulse intensities exceeding $10^7 - 10^8$ photons on the sample per sub-picosecond pulse and prefer less intense pulses spaced by the relaxation time (~0.1 to 10 μs) of the process under investigation. Investigating non-linear dynamics and single pulse imaging experiments require as many as 10^{12} UV/X-ray photons in a single ultra-fast pulse, the duration of which is limited by the ablation time of the sample or by the hydrodynamic expansion time over a resolution element.

It is these large single-pulse intensities that strongly disfavor storage rings with time-gated detectors as an appropriate source for experiments on the 100 fs time scale. Quantum electrodynamics limits the number of photons that an electron can radiate as it travels in its roughly circular orbit in a synchrotron light source to ~ α^{-1} per revolution. Therefore the intensity of the UV/X-ray pulses depends linearly on the stored beam current, I_b, in the storage ring. Likewise, the discrete nature of the radiation of photons as the electron beam bends around the ring leads to the following effects on the electron beam:

1) to spread the energy of the beam around its central value and thereby to increase the bunch length,
2) to increase the beam emittance, ε, (the product of beam size and divergence) as $\varepsilon \sim E^2\Theta^3$ where E is the beam energy and Θ is the bending angle of bend in each achromat of the storage ring lattice.

The spread in beam energy broadens the spectral width of the emitted radiation while the beam size and emittance set the effective source size and divergence of the radiation.

Thus, the current in the electron beam and the emittance of the electron beam determine the average flux on an experimental sample. Both collective instabilities and operating costs put practical limits on the stored current in storage rings. Although the low energy rings in B-factories now operate with ~3 A of stored current, for hard X-ray sources in which minimizing beam emittance is crucial, a more practical means of increasing beam currents above 500 mA and, therefore, time averaged brightness or flux (photons/s/mm^2) may be to use a recirculating linac configuration energy to recover the energy[3] carried by the electron beam rather than the beam itself. The Energy Recovery Linac architecture increases UV/X-ray brightness at most linearly with the electron current; however, the most dramatic increase in the brightness per unit beam current can be obtained through the coherent radiation process that underlies the free electron laser amplifier.

Pulse-to-pulse stability

Stability of both intensity and spectral characteristics is viewed as essential to studies of linear processes, since the radiation pulse will excite only a small fraction of the molecules or materials. Users of third-generation light sources have become accustomed

[3] Energy recovery linacs (ERL) were first proposed by M. Tigner, "A possible apparatus for clashing-beam experiments", *Nuovo Cimento* 37, 1228 (1965).

to 0.1% stability, a level that allows real time subtraction of backgrounds in pump on/pump off experiments.

Pulse duration

Pulses of 20 - 200 fs X-ray pulses are needed to match the characteristic time scales of the dynamic processes under investigation. In the future, users may request[4] pulses as short as 100 attoseconds. Pulse durations on this time scale are far beyond the capabilities[5] of standard synchrotron light sources and are a principal compelling reason to consider linac-based sources for studies of ultra-fast processes.

Even in specially designed storage rings with a suitably isochronous, low momentum compaction[6] lattice, pulse durations would be limited to ~1 ps by coherent synchrotron radiation (CSR)[7]. The CSR[8,9,10,11] can rapidly drain energy from the electron beam, creating an energy chirp from head to tail and increasing beam emittance.

For electron beams with an energy exceeding 1 GeV and with a duration less than 1 ps, carrying 1 nC, CSR can spread the bunch energy by ~1% in a fraction of a single turn. Consequently in the design of an FEL facility dedicated to studies of ultra-fast dynamics (<<1 ps) one is naturally driven to the linac-based free electron laser. Even in such FEL systems, CSR is an important limiting phenomenon in the design of beam bunchers and beam spreaders which direct the full energy beam to different FEL lines.

Timing and synchronization

A large class of experiments (pump-probe) initiate a time-evolving process in the sample with another laser or UV/X-ray pulse. Such pump-probe experiments demand lasers

---

[4] "Now, a new area of experimental physics is emerging, one sufficiently radical to be defined by its own prefix—"attosecond science". By using femtosecond optical pulses to generate wave packets in the soft x-ray region, where wave cycles last for only about 50 attoseconds (as) or 50 x 10-18 seconds, it should be possible to produce multi-cycle x-ray pulses with sub-femtosecond durations. In this issue, Drescher et al. report a first step in this direction. The authors have both created and measured x-ray pulses with durations below the carrier wave period of the original optical pulse." D.T. Reid, "LASER PHYSICS: Toward Attosecond Pulses," Science **291**. No. 5510, 9 March 2001, pp. 1911 – 1913 and M. Drescher, M. Hentschel, R. Kienberger, G. Tempea, C. Spielmann, G. A. Reider, P.B. Corkum, F. Krausz, "X-ray Pulses Approaching the Attosecond Frontier," Science **291**, 1923 (2001).

[5] In storage ring light sources the duration of radiation pulses equals that of the electron bunches, s_z. Once the bunches have circulated for an energy damping time, the quantum nature of synchrotron radiation spreads the electron energy to a value roughly equal to the geometric mean of the beam energy and the critical energy of the synchrotron radiation in the average bending field of the ring. This spread is ~ 10^{-4} to 10^{-3}, causing the injected electron pulses to lengthen to tens of picoseconds. Tuning the lattice of the ring to yield nearly isochronous transport may allow high current bunches with <10 ps duration. In that instance machine operation has been seen to be difficult, unreliable, and incompatible with the needs of most users.

[6] The momentum compaction, usually denoted by α, is the fractional change in orbit length around the storage ring with fractional change in energy beam energy.

[7] CSR occurs when synchrotron radiation with a wavelength roughly equal to σ_z, emitted from the back of electron pulse can propagate through the vacuum chamber to overtake and interact strongly with the head of the pulse as the beam passes through a dipole. See L.I. Schiff, *Rev. Sci. Instr*. **17**, 6 (1946)

[8] "Shielded Synchrotron Radiation and Its Effect on Very Short Bunches", R. L. Warnock, SLAC PUB-*5375*, November 1990

[9] Also M. Dohlus, T. Limberg, "Emittance Growth due to Wake Fields on Curved Bunch Trajectories," *XVIII International Free Electron Laser Conference*, (1996), Rome Italy

[10] J.S. Nodvick and D.S. Saxon, Phys. Rev. **96**, 180 (1954)

[11] E.L. Saldin, E.A. Schneidmiller, and M.V. Yurkov, *Nuc. Inst. Meth. A* 398, 373 (1997)

synchronized[12] to within <20 fs of the UV/X -ray pulse. Other experiments such as single pulse imaging some require no synchronization signal.

Polarization

A dedicated FEL facility should offer complete flexibility to the user in the choice of the polarization of the radiation. Complete right-handed and left-handed circular polarizations are needed for polarization blocking and dichroism experiments.

Pulse repetition rate

Ideally the pulses of radiation should be supplied to the user at a rate limited only by the relaxation times of the processes under investigation. Consequently, rates as high as ~10 MHz are interesting for a large class of experiments. In those experiments that demand single pulse intensity leading to sample damage, the relevant maximum repletion rate will be set by considerations such as how fast the sample can be replaced or annealed.

[12] Ideally the accuracy of synchronization and timing should be an order of magnitude than the X-rat pulse duration. See J. N. Corlett, W. Barry, J. M. Byrd, R. Schoenlein, and A. Zholents, "Synchronization of X-ray Pulses to the Pump Laser in an Ultrafast X-ray Facility", *Proceedings of EPAC 2002*, Paris, France.

III. Physics of Free Electron Lasers

As already discussed in Section I, for strong-field and single pulse experiments that require more than ~10^8 X-ray photons in sub-picosecond pulses, it is not sufficient to rely on the spontaneous, incoherent emission of synchrotron radiation. As quantum electrodynamics limits the radiation from a single electron to ~α photons per radian of bending, controllable amplification of the radiation passing through the undulator is required. With the FLASH FEL[13] at DESY and the LCLS[14] and XFEL[15] under construction at SLAC and DESY respectively spatially coherent sources of soft and hard X-rays seem now to be within reach using the free electron laser mechanism[16] operating in the Self Amplification of Spontaneous Emission (SASE) mode. However, for experiments requiring full spatial and temporal coherence plus femtosecond level timing and synchronization, an alternative FEL architecture that uses a seed laser to initiate the FEL process appears preferred as in the FERMI@Elettra and BESSY FEL projects.

III.A. Basic principles of the FEL

The basic principle of the high gain free electron laser[17,18] is both well known and tested experimentally in numerous experiments at wavelengths from the millimeter waves to ~ 100 nm. The best known and first tested instance of a free electron laser operating with high single pass gain was the master oscillator-power amplifier configuration that was demonstrated in experiments[19] by a joint Lawrence Berkeley- Lawrence Livermore

---

[13] "FLASH is a user facility providing laser-like radiation in the VUV and soft X-ray range to various user experiments in many scientific fields. It is also a pilot facility for the future XFEL." http://vuv-fel.desy.de/

[14] The LCLS homepage is http://www-ssrl.slac.stanford.edu/lcls/.

[15] The European X-Ray Laser Project XFEL, http://xfel.desy.de

[16] For a reference to FEL activities around the world including recent experimental progress toward demonstrating FELs at short wavelength, see http://sbfel3.ucsb.edu/www/vl_fel.html

[17] The free electron laser was first proposed by John Madey in 1971; see J.M.J. Madey, J. Appl. Phys., **42**, 1906 (1971). Madey's concept was itself predated by similar concepts for the amplification of microwave radiation; R.M. Philips, IRE Trans. Electron Devices, **7**, 231 (1960). Madey and his co-workers demonstrated both the operation of an FEL amplifier and an FEL oscillator. L.R. Elias, W.M. Fairbank, J.M.J. Madey, H.A. Schwettman and T.I. Smith, Phys. Rev. Lett. **36**, 717 (1976) and D.A.G. Deacon, L.R. Elias, J.M.J. Madey, G. J. Ramian, H.A. Schwettman and T.I. Smith, Phys. Rev. Lett. **8**, 892 (1977).

[18] Early analyses of the systematics of the FEL process including the derivation of the high gain regime are given in A Bambini, A. Renieri, S. Stenholm, "Classical theory of the free electron laser in a commoving frame", Phys. Rev. A, Vol. 19, n.5, (1979) and W.H. Louisell, J.F. Lam, D.A. Copeland, W.B. Colson, "Exact classical electron dynamic approach for a free-electron laser amplifier", Phys. Rev. A, col. 19, n.1, (1979). Another important early analysis was given by N.M . Kroll, P.L . Morton and M.N . Rosenbluth, IEEE J. Quantum Electron. **QE 17** (1981) 1436. It was this latter paper that provided the basis of the computer model for designing the first successful high gain experiment.

[19] The LBNL-LLNL experiment called ELF (Electron Laser Facility) was aimed at showing that long (~50 ns), high current pulsed could be transformed into very high power, high frequency microwaves that would be used to drive a high gradient rf-accelerator structure at more than 100 MeV/m for a TeV linear collider. This Two-Beam Accelerator (TBA) concept was invented by A.M. Sessler, who conceived of ELF as the first stage in the realization of the TBA. See A. M. Sessler, "Laser Acceleration of Particles," AIP Conf. Proc. 91, 154-159 (1982).
Other early experiments at low wavelengths include D.A. Kirkpatrick, G. Bekefi, A.C. DiRienzo, H.P. Freund, and A.K. Ganguly, "A Millimeter and Submillimeter Wavelength Free-Electron Laser," Phys.

Laboratory collaboration in the mid-80's. While these experiments were performed at a wavelength of 8 mm (35 GHz) in the presence of a waveguide, they verified all the basic predictions of the 1-dimensional theory formulated by Bonifacio, Pellegrini and Narducci[20] modified to include waveguide effects.

In traversing a undulator – a periodic magnetic field device (or structure) - an electron bunch with a relativistic factor, γ, radiates at a wavelength (in the beam frame) that is the back scattered value, λ_w/γ, of the Lorentz contracted period, λ_w of the static magnetic field of the undulator. To the observer in the laboratory frame, the radiation is Doppler upshifted by a factor $2\gamma/(1+\theta^2_{rms})$, where θ_{rms} is the rms angle by which the electrons bend in the undulator.

Since the electrons will have an rms transverse velocity in the undulator, the longitudinal velocity is reduced such that the radiation emitted in the forward direction will slip forward with respect to the beam. If the electrons oscillate in phase with the field, they will continually lose energy to the field leading to the FEL instability. This resonance condition is that the electrons slip one optical period per undulator period. Thus, the resonance condition among the radiation wavelength, λ_r, the undulator[21] wavelength and the energy of the electrons is

$$\lambda_r = \frac{\lambda_w}{2\gamma^2}\left(1 + K^2_{rms}\right) \qquad (1)$$

where $K_{\rm rms}$ equals $K/\sqrt{2}$ (= a_w) for a planar undulator and equals K for a helical undulator; $\gamma m_e c^2$ is the energy of the electron beam. The dimensionless vector potential of the undulator field, K, is determined by the maximum magnetic field on axis, B_w and the undulator period, λ_w. In physical units,

$$K = 0.934\ \lambda_w[\text{cm}]\ B_w[\text{T}]. \qquad (2)$$

III.A.1. Gain & bunching

The basic functional mechanism of the FEL, as described in the 1-dimensional (1-D) theory, is a collective instability of the electron bunch as it traverses a periodic magnetic field structure. At the beginning of the process, the initial radiation (either from a master oscillator or from the incoherent spontaneous synchrotron radiation) induces an energy modulation (micro-bunching) in the bunch that is converted to a density modulation at the radiation frequency. The fraction, f, of the electrons in the "micro-bunch" radiate coherently with intensity proportional to N_e^2(where N_e is the number of electrons). The

---

Fluids B **1** (1989) 1511. Also, D.A. Kirkpatrick, G. Bekefi, A.C. DiRienzo, H.P. Freund, and A.K. Ganguly, "A High Power 600 mm Wavelength Free-Electron Laser," Nucl. Inst.. Meth. A **285** (1989) 43.

[20] R. Bonifacio, C. Pellegrini, and L. Narducci, Optics Comm. **50**, 373 (1984), hereinafter BPN. An excellent elaboration of the basics of free electron laser theory is presented in the review article, R. Bonifacio et al., La Rivista del Nuovo Cimento, **13**, N. 9, (1990). Another lengthy exposition from first principles is E. L. Saldin, E.A. Schneidmiller, M.V. Yurkov, "The physics of free electron lasers. An introduction," Physics Reports, **260**, Issue 4-5, (1995) 187-327

[21] While insertion devices frequently use the word "undulator" for K≤1 and use "wiggler" for K>1, this paper uses the word undulator for all values of K. Note that in FELs K > 1 are strongly preferred.

coherent radiation augments the incident radiation (or initial noise signal) further increasing the micro-bunching leading to yet more coherent radiation. As the electrons and the radiation propagate together down the undulator, the result is an exponentially growing radiation field with a power that grows as

$$P = aP_n e^{z/L_g} \tag{3}$$

In equation (3) P_n is the initial signal strength, α is a coupling coefficient between the signal strength and the dominant mode, *and z* is the distance along the undulator. L_G is the gain length, that is, the distance for an e-folding of the radiation intensity.

In particular, when an electron beam traverses the undulator with a period, λ_w, synchrotron radiation is generated at the resonant wavelength, λ_r. As the signal grows, the pondermotive potential, created by the undulator field and the radiation field, bunches the electrons periodically on the wavelength scale of the resonant (sometimes called optical) wavelength. The current compression due the free electron laser action can be computed from the bunching parameter, b, which is the ensemble average

$$b = \left| \left\langle e^{iq_j} \right\rangle \right| \tag{4}$$

where θ_j is the phase of the j^{th} electron with respect to the radiation frequency. For an unbunched beam b = 0 while for a beam bunched to a delta function of current b = 1. The strong FEL bunching is evidenced by the fact that when the gain saturates, the bunching factor reaches a maximum $b_{max} \sim 0.8$ regardless of the actual values of the initial current, λ_w, or λ_r. Bunching on the scale of an optical wavelength is clearly seen in the GENESIS simulation (Figures 4 and 5) from the DESY Technical Design Report.[22]

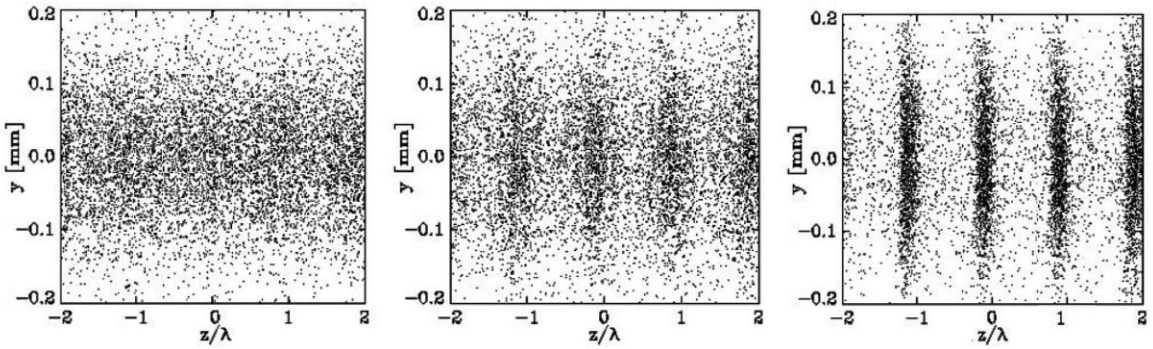

Figure 4. GENESIS calculations of particle positions in the transverse direction y and in z at three locations along the undulator. Left panel is at the entrance to the undulator; the right panel is at saturation. The central panel is at an intermediate position.

[22] TESLA Technical Design Report, Part V, The X-Ray Free Electron Laser, Editors: G. Materlik Th. Tschentscher, p.25 http://tesla.desy.de/new_pages/TDR_CD/PartV/fel.html (2001)

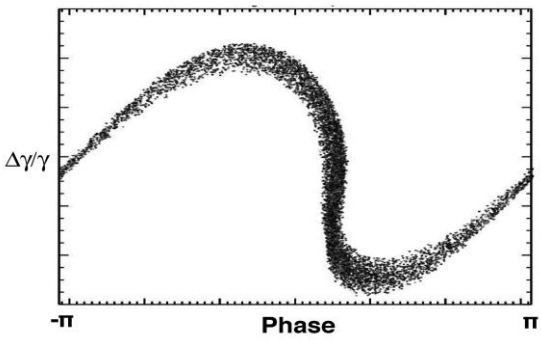

Figure 5. GENESIS calculation[23] of the longitudinal phase space at the location of maximum bunching

The gain of the FEL and the speed of the bunching process in a cold (zero emittance) beam with no incoherent energy spread is described by the BPN universal scaling parameter[24], ρ;

$$r = \left(\frac{a_w w_p}{8 c k_w}\right)^{2/3} \mu \frac{I^{1/3} B_w^{2/3} k_w^{4/3}}{g} \tag{5}$$

where ω_p is the relativistic plasma frequency, a_w is the dimensionless vector potential of the undulator and k_w is the undulator spatial frequency.

$$a_w \approx 0.66\, B_w(\text{Tesla})\, \lambda_w(\text{cm}) \tag{6}$$

$$k_w \approx \frac{2\pi}{\lambda_w} \tag{7}$$

and

$$w_p^2 = \frac{4\pi n_e r_e c^2}{g^3} \tag{8}$$

In equation (8) n_e is the electron density and r_e is the classical radius of the electron. The electron density is related to the beam radius r_b and the beam current by

$$I = \pi c e n_e r_b^2 \tag{9}$$

The e-folding (gain) length, L_G, for the power carried by the electromagnetic field as computed from the 1-dimensional theory is given by the general expression,

[23] Figure 5 is extracted from presentation by S. Becker, "Table-top Free Electron Laser," (2006)

[24] BNP paper. In this paper, the authors graciously refer to this parameter as the Pierce parameter due to its similarity to a parameter in microwave tube theory. It is also referred to in the literature as the universal FEL parameter. The present authors have used the term BNP parameter recognize the first introduction of this parameter in the FEL analysis.

$$L_G = \frac{l_w}{4\pi\rho\ \mathrm{Im}(2\mu)} \qquad (10)$$

where Im(μ) is the solution to the (cubic) eigenvalue equation for the FEL instability written for the field intensity. In the cold-beam, 1-D limit, Im(μ) = $\sqrt{3}/2$.

The line width, $\Delta\lambda_□/\lambda_□$, of the output radiation from the SASE process in the classical regime is the root mean square of the homogeneous and inhomogeneous broadenings. The homogeneous width is equal to ρ and is related to the temporal spikes that characterize SASE output. Inhomogeneous broadening arises from errors in the beam energy, undulator field and undulator wavelength; their contribution to $\Delta\lambda_□/\lambda_□$ can be found by differentiation of the resonance condition.

Another experimentally verified feature of the high gain FEL is that the rate of the bunching action is proportional to $\rho\lambda_w$. Hence bunching actually proceeds more rapidly as the input current increases. It is this characteristic that makes the FEL buncher[25,26] so attractive in comparison with other bunching schemes when the final peak value of the bunched current must be extremely large or when the bunch length must be very short.

Yet another feature of the FEL that compares favorably with respect to other bunching schemes is that the length over which bunching occurs scales favorably (increases only linearly with increased beam energy). The FEL action does, however, induce an energy spread in the beam that is proportional to the gain. By terminating the undulator before the FEL process saturates one can a) maximize current multiplication, b) keep the induced energy variation small, and c) minimize the length of the undulator. All of these considerations play actively in the design of both FEL bunchers and high-gain harmonic generation (HGHG) systems such as the FERMI FEL (to be described in detail later)..

III.A.2 Limitations on the FEL process

As the electron beam characteristics depart from the cold beam limit, the rate of the FEL bunching process, and consequently the FEL gain, can be strongly and adversely affected. Specifically if the spread in longitudinal velocities $\langle v_z \rangle$ of the beam electrons is so large that the longitudinal drift of electrons is a large fraction λ_r as the beam propagates, the gain will be strongly suppressed. The spread, $\langle v_z \rangle$, at the entrance to the undulator arises from the incoherent energy spread in the beam $\Delta\gamma/\gamma$ and from the beam

[25] H. D. Shay, et al., "Use of a FEL as a Buncher for a TBA Scheme, " Proc. of the Int. FEL Conference, (Paris, 1990).

[26] W. A. Barletta, R. Bonifacio, P. Pierini et al, "An rf-linac, FEL buncher," Nucl. Inst. And Meth. A, 329, Issues 1-2, 1993, pp. 348-360. This concept was applied to the generation of femtosecond X-ray pulses in W. A. Barletta, R. Bonifacio, P. Pierini, "High brilliance, femtosecond x ray sources with FEL assist," Proc. of 4th Generation Light Sources Workshop, Stanford, CA, 24-27 Feb. 1992, SSRL Report 92/02 " We describe EFSX … to produce multi-kiloampere pulses … in the generation of extremely short bursts of X-rays. The key technical concept, the *use of the free electron laser as a bunching mechanism* … As laser photo-cathode sources of beams evolve to yield ever better emittances, the EFSX could be easily retrofitted *to furnish the drive beam for an efficient x ray free electron laser.*" These early ideas matured into the ESASE concept discussed later in this review.

emittance, ε. We expect the FEL to be insensitive to energy spreads and variations as long as

$$r_1 = \frac{4}{\rho}\frac{\Delta\gamma}{\gamma} < 1 \tag{11}$$

To satisfy the high gain FEL conditions, the phase area of the electron beam should be smaller than that of the diffraction-limited radiation; i.e.,

$$r_2 = \frac{4\pi\varepsilon_n}{\lambda_r g} < 1 \tag{12}$$

where ε_n is the normalized emittance of the electron beam. In optical FELs using fine, very low emittance beams the gain can be reduced and the rate of bunching will be decreased if the radiation diffracts out of the electron beam too rapidly. Specifically the Rayleigh range of the radiation should exceed L_G; i.e.,

$$r_3 = \frac{L_G}{Z_R} < 1. \tag{13}$$

The constraints (11), (12), (13), and the resonance condition (1) are not all independent. One can easily show that

$$r_1 = \frac{1}{4} r_2^2 r_3 \tag{14}$$

The sensitivity of the FEL gain function Im(μ) to the variations in beam emittance and energy spread can be characterized[27] in terms of these dimensionless parameters. The results for the case of weak and strong diffractive effects (small and large r_3) are shown in Figure 6.

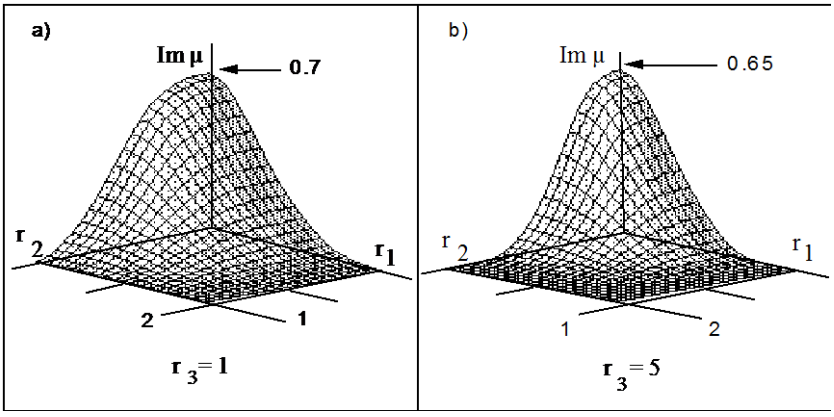

Figure 6. Gain surface, Im μ, versus scaled emittance and energy spread for two values of the diffraction parameter, r_3

[27] W. A. Barletta, A. M. Sessler, L-H Yu, "Physically transparent formulation of a free-electron laser in the linear gain regime," Nucl. Inst. and Meth. A331 (1993) 491-495); Figure 6 is reproduced from this paper. The analysis of this paper is based on a numerical model and fitting of earlier analyses of L.-H. Yu, S. Krinsky, and R. L. Gluckstern, Phys. Rev. Lett. **64**, 3011 (1990) and of Y.-H. Chin, K.-J. Kim, and M. Xie, LBL Report 30673 (Sept. 1991)

III.A.2.a Space charge effects

In multi-kiloampere beams at relatively low energy (<100 MeV), the debunching effects of longitudinal space charge forces can compete with the bunching action of the FEL process. The longitudinal space charge force, F_{sc}, varies as $\gamma^{-1/3}$; therefore, in GeV beams it is completely negligible in the FEL process. Although space charge waves driven by coherent synchrotron radiation can filament the longitudinal phase space in bunch compressors as described in Section IV.D.

To evaluate the effects of space charge at low beam energy it is not sufficient to consider the free space action of F_{sc}; one must include space charge in the pendulum equation that governs the FEL instability. In their analysis[28], Murphy, Pellegrini and Bonifacio find that the FEL process tends to be stabilized by space charge terms that are proportional to $4\rho(1+K^2/2)/ K^2$; hence, they conclude, the space charge effects at resonance are negligible for systems with $\rho < 0.01$. They also find that unlike the case without space charge, there is a lower negative value of detuning $(\gamma-\gamma_r)$ beyond which the process is stabilized (no growth of the FEL signal).

A fundamental physical argument also provides a condition under which space charge effects are negligible; i.e., the FEL gain length (computed without space charge) should be much less that the plasma wavelength, λ_P. Equations (5), (8), and (10) imply that

$$K >> \frac{1}{3^{3/4}\pi^2 2^{3/2}}\left(\frac{\Omega_p \lambda_o}{c}\right)^{1/2} \approx 1.5\times 10^{-2}\left(\frac{\Omega_p \lambda_o}{c}\right)^{1/2}. \qquad (15)$$

III.A.3 Initiation of the FEL process

FEL amplifiers can start operation by amplifying the incoherent shot noise[29] that is spontaneously radiated[30,31] by the electrons in the beam as they enter the undulator. As the electron beam and the radiation co-propagate through the undulator, the radiation slowly slips through the electron beam in accordance with the resonance condition and the radiation power grows exponentially. This process, called Self Amplification of Spontaneous Emission (SASE), results in a high power output with very large temporal fluctuations in the radiated power during the pulse. For single-shot experiments, and those that do not require temporal coherence, such very high power pulses are ideal for studying non-linear effects in materials. SASE sources, however, may be inconsistent with the characteristics of the radiation demanded by experiments that require a high degree of pulse-to-pulse temporal reproducibility or a high degree of temporal coherence.

[28] J. B. Murphy, C. Pellegrini and R. Bonifacio, "Collective Instability of a Free Electron Laser including Space Charge and Harmonics," Optics Comm. **53**, no.3, p. 197 – 202, (1985)

[29] Shot noise is the term that describes the random statistical fluctuations in the incoherent synchrotron radiation due to the random arrival time of the electrons in the beam. The phenomenon is intrinsically quantum mechanical as the beam current is carried by a finite number of quanta (electrons). See http://qwiki.caltech.edu/wiki/Shot_Noise

[30] "Spectrum, temporal structure, and fluctuations in a high-gain free-electron laser starting from noise", R. Bonifacio, L. D. Salvo, P. Pierini, N. Piovella, C. Pellegrini, Physical Review Letters, **74**, pp. 7073, (1994)

[31] "Shot Noise Startup of the 6 nm SASE FEL at the TESLA Test Facility", P. Pierini and W.M. Fawley, Proceedings of the 17th Int. Free Electron Laser Conf. Nucl. Instr. Methods Physics Res. A375 (1995)

The large fluctuations in the SASE process are nicely illustrated in Figure 7a, which displays experimental results[32] from the Tesla Test Facility FEL (now FLASH). The calculated temporal structure of X-ray FELs that start from shot noise is illustrated in Figure 7b. Direct measurements of such behavior are presently beyond experimental capabilities.

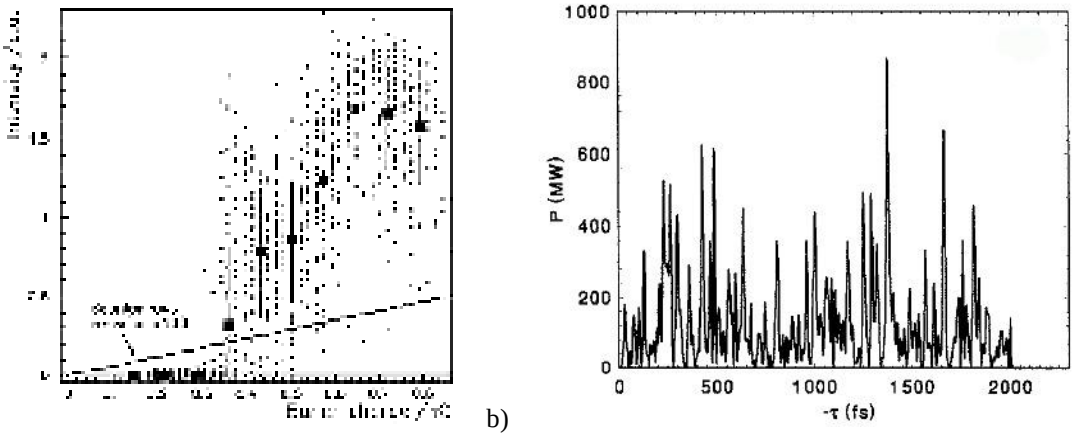

Figure 7 a) "SASE intensity versus bunch charge measured at TTF FEL. The straight line is the spontaneous intensity multiplied by a factor of 100. To guide the eye, mean values of the radiation intensity are shown for some bunch charges (dots). The vertical error bars indicate the standard deviation of intensity fluctuations, which are due to the statistical character of the SASE process." b) 1-D simulation the temporal structure of a "typical" SASE FEL in the EUV at saturation from Saldin et al.[33]

In the cold beam limit, the homogeneous line width of the SASE output is ~ρ. Effects such as magnetic field errors, beam misalignments and energy fluctuations within the pulse will lead to inhomogeneous broadening of the line width by am amount calculable from the derivatives of the resonance condition with respect to the relevant variable.

Recently, Bonifacio, Piovella and Robb have shown[34] that if the mean number of photons emitted per electron (at saturation) is much less than one, strong quantum effects modify the output of the FEL. Quantitatively, they introduce a parameter[35], ρ′, defined as the

[32] Figure 5a and caption are taken from J. Andruszkow et. al., "First Observation of Self-Amplified Spontaneous Emission in a Free-Electron Laser at 109 nm Wavelength," Phys. Rev. Lett., Vol. 85, Num. 18, p. 3825, 30 October 2000. See also M.J. Hogan, C. Pellegrini, J. Rosenzweig, G.A. Travish, A. Varfolomeev, S. Anderson, K. Bishofberger, P. Frigola, A. Murkoh, N. Osmanov, S. Reiche, and A. Tremaine, "Measurements of High Gain and Intensity Fluctuations in a SASE FEL," Phys. Rev. Lett. **80** (2) (1998) 289.

[33] E. L. Saldin, E. A. Schneidmiller and M. V. Yurkov, "Statistical properties of radiation from VUV and X-ray free electron laser," Opt. Comm., **148**, Issues 4-6, (1998), 383-403.

[34] R. Bonifacio, N. Piovella, G. Robb, R. Bonifacio, N. Piovella, G. R. M. Robb, Nucl. Inst and Meth. A **543**, 645 (2005); R. Bonifacio, "Quantum SASE FEL with laser wiggler ," Nucl. Inst. and Meth. A, **546**, 3, p. 634-638 (2005)
See also N. Piovella, G.R.M. Robb, "Quantum theory of SASE FEL," **A** 543 (2005) 645–652

[35] This parameter was first introduced by R. Bonifacio, F. Casagrande, Opt. Comm. **50**, 251 (1984) and R. Bonifacio, F. Casagrande, Nuc. Inst and Meth. A **237**, 168 (1985). Another early formulation of a quantum mechanical theory of the FEL was published by G. Preparata, "Quantum Field Theory of the Free Electron Laser", Phys. Rev. A, **38**, (1988). Other quantum mechanical descriptions of the FEL process have been published by E. M. Belenov, S. V. Grigorev, A. V. Nazarkin, and I. V. Smetanin, JETP **78**, 431 (1994) and

usual FEL parameter, ρ, times the ratio of the electron energy and the photon energy. Moreover, ρ′ represents the maximum number of photons emitted per electron. The classical FEL regimes occurs when ρ′ >>1. They prove that when ρ′< 1 the broad superposition of chaotic series of random spikes that characterizes SASE shrinks to a very narrow spectrum of emitted radiation with extremely high peak power as shown in Figure 8[36]. The nature of the transition from the classical regime to the quantum regime can be seen in Figure 8c, which shows the imaginary part of the unstable root of the cubic equation that describes the FEL gain in the 1-D limit as a function of the energy detuning parameter, $\bar{d} = (g_o - g)/r g_o$.

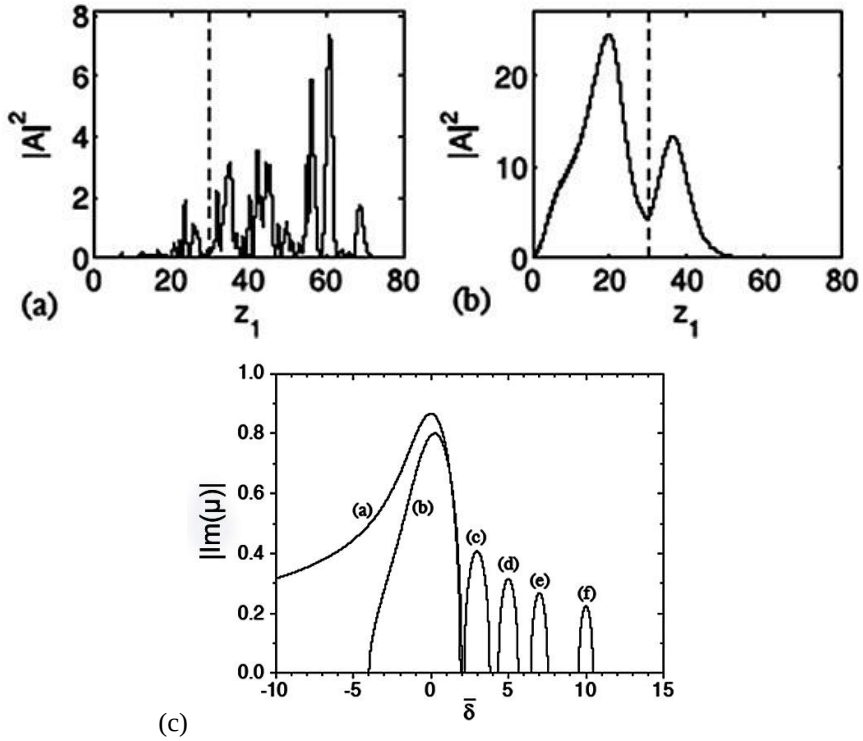

Figure 8[37]. Numerical solutions 1-D FEL field equations in the classical and quantum regimes: Graphs (a) and (b) show the scaled field intensity $|A|^2(z_1)$ after 50 gain lengths when the system evolves classically ρ´ = 5 and quantum mechanically ρ´ = 0.05, respectively. z_1 is the retarded time. Graph (c) The imaginary part of the unstable root of the cubic equation v. $\bar{d}$; for $1/\bar{r} = 0$; (a) 0.5, (b) 3, (c) 5, (d) 7, (e) and 10, (f).

Unfortunately the predicted gain lengths in the quantum regime are impractically long, unless the FEL undulator is itself intense electromagnetic radiation. Indeed, Bonifacio has proposed[38] just such a scheme to test quantum SASE. While these ideas are intriguing

---

C.B. Schroeder, C. Pellegrini, P. Chen, Phys. Rev. E **64**, 056502 (2001). However these earlier papers do not treat the peculiar characteristics of SASE systems operating deep in the quantum regime.

[36] Id.

[37] Id.

[38] R. Bonifacio, "Quantum SASE FEL with laser undulator," Nucl. Inst. and Meth. 546 (3), pp. 634-638 (2005)

conceptually, present day FEL facilities must be based on classical FELs with conventional undulator magnets.

The practical alternative to produce narrow bandwidth, temporally coherent soft X-ray radiation from an FEL is to use a master oscillator-driven, power-amplifier configuration. In this configuration the temporal coherence is determined by the properties of the master oscillator or seed laser. Sincrotrone Trieste has adopted this approach implemented in its FERMI @ Elettra project. The main requirement for the seed laser is to deliver sufficiently high peak power (~100 MW) in the UV, at wavelengths tunable over a rather large range, 240-360 nm, with variable pulse duration as required by the scientific application program of the FEL facility. For the FERMI FEL this range is 100 fs to 1 ps.

Obviously, all input laser characteristics – particular the central wavelength – must be as stable as practically obtainable. Moreover the timing jitter must be small compared with the pulse length of the laser output.

III.A.4. Output power and saturation

As the electrons and the radiation propagate through the undulator, the radiation power grows exponentially as

$$P(z) = P_o e^{z/L_G} < P_{sat} \tag{16}$$

until the power approaches its saturation value, P_{sat} after passing a distance Z_{sat} through the undulator. The initial power is the integrated shot noise incoherently radiated into the dominant growing mode by the electrons passing through the first gain length. In the 1-D limit, the noise power[39] is

$$P_o \gg \frac{r^2 c E_{beam}}{l_r}. \tag{17}$$

In the 1-D, cold beam limit (ideal beam) the output power at saturation is determined by the FEL scaling parameter ρ;

$$P_{sat,1\text{-}D} = \rho P_{beam} \tag{18}$$

Simulations[40] with the simulation code GINGER show that this value is a conservative estimate of the shot noise from a non-ideal beam. In the presence of strong 2-dimensional effects, the corresponding expressions[41] for the output power of the FEL at saturation given are not as easily interpreted. One can, however, rewrite these expressions in a form more readily understood in terms of the predictions of the 1-dimensional theory. In particular the *approximate* expression of Chin, Kim, and Xie reduces to

[39] M. Xie, "Design Optimization for an X-Ray Free Electron Laser Driven by SLAC Linac," Proc. IEEE Part. Accel. Conf. (1995)
[40] W.M.Fawley et al., Proc. IEEE Part. Accel. Conf. (1993), 1530
[41] L.-H. Yu, S. Krinsky, and R. L. Gluckstern, Phys. Rev. Lett. **64**, 3011 (1990) and Y.-H. Chin, K.-J. Kim, and M. Xie, LBL Report 30673 (Sept. 1991) and Proceedings of the FEL 1991 Conference, Santa Fe, NM

$$P_{sat;2\text{-}D} = \left(\frac{\mathrm{Im}(\eta)}{\sqrt{3}/2} \right)^4 \rho \, P_{beam} \qquad (19)$$

Simulations with the code GINGER indicate that the exact expression for the power at saturation in the presence of strong 2-D effects is far more complicated in its dependence on the r_i than indicated in equation (19).

Once the FEL process reaches saturation, the electron beam begins to absorb energy from the radiation field. In an intuitive, physical sense once the average energy of the beam has been decreased by ρE_o the beam will have fallen out of the gain-bandwidth (ρ) of the FEL. In detail, as the radiated power begins to approach saturation (roughly after the bunching parameter b reaches its maximum value of ~0.7 – 0.8 at ~0.8 Z_{sat}), in an undulator with K>1 the electron beam begins to lose energy linearly as it propagates down the undulator. The energy extraction process can be continued beyond Z_{sat}, if K is decreased so to keep the amplifier in resonance. This process is known as tapering.

The effectiveness of tapering was demonstrated[42] in the LBNL-LLNL microwave FEL in 1986. Without tapering the electrons will linearly recover energy back from the radiation field until they are once again within the gain-bandwidth of the amplifier. Both cases are illustrated in the calculation[43] shown in Figure 9 for the LEUTL amplifier.

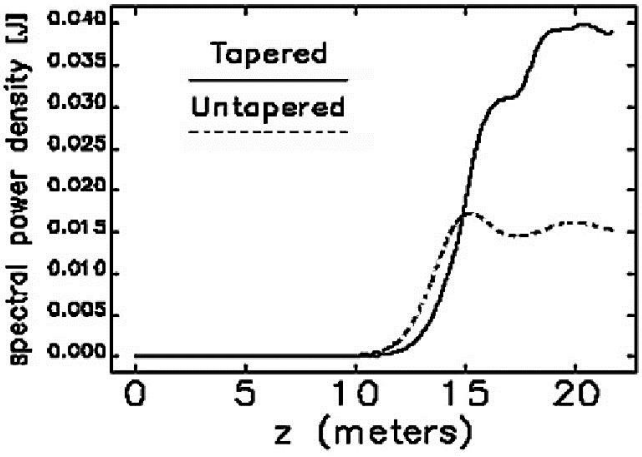

Figure 9. The effects of tapering of the LEUTL undulator

III.A.5 Slippage effects

The results described in the previous sections describe the behavior of a beam in which the effects of the difference in velocity between the electrons and light are insignificant. Quantitatively, this approximation applies when the length of the electron bunch, L_b is much greater than a cooperation length, L_c. Recalling that the radiation slips ahead of the

[42] T.J. Orzechowski, et al., Phys. Rev. Lett. **57** (1986) 2172.

[43] Figure 9 is reproduced from W. M. Fawley, Z. Huang, K-J, Kim, and N. A. Vinokurov, "Tapered undulators for SASE FELs," Nucl. Inst. and Meth. A **483**, Issues 1-2 , (2002) 537-541

electrons by one optical wavelength per undulator wavelength, one defines L_c as the length of the bunch over which the radiation slips in one gain length. Hence,

$$L_c = (L_G/\lambda_w)\lambda_r . \tag{20}$$

Even in beams that are many cooperation lengths long, the effects of slippage can be seen in the temporal characteristics of SASE FELs at saturation. The output typified by the calculation of Figure 3b, shows that the amplified noise signals are correlated only over a duration of $\sim L_c/c$. Fourier analysis of such a temporal signal yields a bandwidth for the SASE FEL of $\Delta\lambda/\lambda \approx \rho$ as previously noted.

In their analysis of the behavior of the FEL in bunches of finite length Bonifacio and Casagrande[44] introduce a superradiance parameter K_s, which is the ratio between the cooperation length and the bunch length:

$$K_s = \frac{L_c}{L_b} = \frac{l_r}{4\pi r L_b} \tag{21}$$

The parameter K_s describes the interplay between gain and slippage. For $K_s << 1$, the FEL is operating in the long bunch (steady state regime); slippage does not affect the gain length. In contrast when $K \geq 1$, the FEL is in the strong slippage, weak super-radiant regime[45] in which the number of periods per gain length is much greater than the number of optical wavelengths in the electron bunch, N_b. Slippage has a significant effect in suppressing gain. Even in this regime the beam is bunched by the radiation reaction on the electron bunch. The peak value of the bunching parameter is slightly lower (≈ 0.60) and the gain length is somewhat larger than in the steady state regime. Note that if the bunch length is shorter than the cooperation length, there is no difference between uniform excitation of the FEL process and SASE startup; both display a soliton-like solution to the FEL equation.

The gain after a distance z in the undulator is

$$G_{SR} = \left(\frac{2\pi r}{l_w} z\right)^{2/3} \tag{22}$$

In the limit in which the bunch is one optical wavelength long, the super-radiant gain length is about three times the steady state, L_G. The free electron laser has never been tested in this extreme strong slippage limit.

III.B. Design of SASE X-ray sources

For producing radiation from 10 eV to 1 keV, electron beams with energy in the range of 1 - 3 GeV can drive a SASE FEL using undulators 15 – 40 m long. Two such facilities

[44] R. Bonifacio amd F. Casagrande, "Classical and Quantum Treatment of Amplifier and Superradiant Free-Electron Laser Dynamics," J. Opt. Soc. America B: Optical Physics ***2*** **(1)**, pp. 250-258

[45] R. Bonifacio, F. Casagrande, C. Cerchioni, L. de Salvo-Souza, P. Pierini, and N. Piovella, "Physics of the High Gain FEL and Super-radiance" La Rivista del Nuovo Cimento, (1990).

are the SPring-8 Compact SASE Source (SCSS)[46] in Japan and the VUV-FEL[47] (now FLASH) in Germany. Both facilities employ high gradient accelerator technologies developed for linear colliders, C-band, traveling wave, room temperature linacs in Japan and superconducting rf-linacs at DESY. FLASH is a soft X-ray user facility testing SASE operation at ~200 eV and has begun an active user program. It will be a very important step on the way to realizing hard X-ray FELs.

Using sufficiently low emittance, 10 - 15 GeV electron beams passing through 100 meter long undulators, one can produce sub-picosecond pulses of 8 - 12 keV X-rays with a peak brightness nine orders of magnitude higher than obtainable from the best third generation storage rings. The Linac Coherent Light Source project (LCLS) at SLAC is on a path to operate such a machine in 2008 initially as an exploratory facility and soon thereafter as a user facility. The DESY laboratory in Germany has proposed a similar project[48], XFEL, with a fully developed set of user beamlines. Although XFEL was originally proposed in association with the proposed TESLA superconducting linear collider project it is now a stand-alone project.

While the demonstration of saturated SASE in a high gain FEL was first demonstrated in the mid-1980s in the ELF experiment[49] conducted by the Lawrence Berkeley and Lawrence Livermore National Laboratories, fully convincing experimental evidence that this approach could be extended to the UV and beyond were not in hand for more than another decade[50]. A notable step[51] aimed at exploring the practicality of the SASE

[46] "SCSS is an abbreviation for SPring-8 Compact SASE Source. This is a soft X-ray radiation facility based on a SASE-FEL. SCSS is designed "compact" by means of (1) Short-period in-vacuum undulator, and (2) high-gradient C-band accelerator. Whole system including the electron beam injector, C-band accelerator and the undulator fits within 100 m long facility." In contrast with other SASE facilities, in SCSS a "high-voltage pulsed gun with single crystal thermionic cathode is employed. This is because, this system does not require a short pulse laser system which is sometimes troublesome, and needs manpower to maintain. For the cathode material, we will use CeB6 cathode. It is a single crystal cathode, which maintains a very flat cathode surface after usage of cathode at high temperature by evaporation of cathode material."
T. Shintake, T. Tanaka, T. Hara, K. Togawa, T. Inagaki, Yujong Kim, T. Ishikawa, H. Kitamura, H. Matsumoto, S. Takeda, M. Yoshida, Y. Takasu, "Status of SCSS: SPring-8 Compact SASE Source Project", *Proceedings of the Eighth European Particle Accelerator Conference*, 2002, Paris, France
See also http://www-xfel.spring8.or.jp/SCSS.htm

[47] V. Ayvazyan et al. "First operation of a free-electron laser generating GW power radiation at 32 nm wavelength," Eur. Phys. J. D **37**, 297–303 (2006). "The electron bunches are produced in a laser-driven photoinjector and accelerated to 445 MeV by a superconducting linear accelerator. Bunch charges between 0.5 and 1 nC are used. At intermediate energies of 125 and 380 MeV the electron bunches are longitudinally compressed, thereby increasing the peak current from initially 50−80 A to approximately 1−2 kA as required for the FEL operation. The 30 m long undulator consists of NdFeB permanent magnets with a fixed gap of 12 mm, a period length of λ_u = 27.3 mm and peak magnetic field B_u = 0.47 T. Finally, a dipole magnet deflects the electron beam into a dump, while the FEL radiation propagates to the experimental hall." Hereinafter, DESY32.

[48] TESLA-Technical Design Report, DESY 2001-011, ECFA 2001-209, CDROM, March 2001. See http://tesla.desy.de/new_pages/tdr_update/start.html

[49] T. Orzechowski et al., Phys. Rev. Lett. 54, 889 (1985). The gain precisely measured was the highest ever seen in a free electron laser, nearly one-folding in power every undulator period.

[50] In the late 1980s the generously funded FEL programs at LLNL and at Los Alamos were shortsightedly diverted away from explorations of fundamental FEL physics well within their reach toward "mission-specific" R&D aimed at producing multi-MW average power FELs for ballistic missile defense. With the demise of these defense programs, experimental investigations into the details of the SASE process and its

architecture for generating short wavelength radiation for a linac-based, fourth-generation[52] light source was provided by the LEUTL experiment[53,54] conducted at Argonne National Laboratory.

LEUTL was specifically designed with a primary goal of studying the physics and technology of high-gain SASE FELs relevant to linac-based, fourth-generation light sources. Consequently, the operating range of LEUTL was chosen to be from 530 nm down to 120 nm. An especially important part of the LEUTL studies was the experimental verification of the dependence of FEL scaling relationships on output wavelength. Relationships of critical interest included the variation of gain length and saturation output power with changes in beam parameters such as beam current and emittance. Accurate comparison of analytical and computational predictions with measurements of such relationships required operation of the FEL that was highly controllable and stable over long periods of time. The strong dependence of gain on beam current plus the strong sensitivity of FEL gain to beam emittance required great attention to the use of bunching chicanes to increase the peak current without degrading beam emittance. The LEUTL experiment provided excellent experimental evidence concerning deleterious effects of CSR induced in the chicane on beam emittance.

The first successful program to create a VUV/X-ray FEL user facility is built on the groundbreaking program[55] in SASE FELs conducted using the superconducting rf linac, the TESLA Test Facility, first built for linear collider research. In 2002, DESY team reported[56] the first example of saturated FEL output at a wavelength below 100 nm using the 250 MeV TESLA Test Facility (TTF) beam. The growth of the radiation power shown in Figure 10a reproduced from their report shows clear saturation and excellent agreement with computational simulations. Also of great significance was the extremely short bunch length, 50 fs, putting SASE systems well on the way to providing useful EUV beams to users. Most recently, the DESY group has reported[57] GW operation of their FEL at 32 nm making possible the first major user program at an FEL facility. An example of the spectral output is shown in Figure 10b. The great variation of the three curves in Figure 10b exemplifies the chaotic nature of the SASE process. That behavior is quantified in Figure 10c which demonstrates that the measured probability distribution

---

statistical nature had to wait until the late 1990s and the strong interest in constructing X-ray FELs as fourth-generation light sources.

[51] A second, contemporaneous experiment in the US conducted at near IR wavelengths was VISA – a collaboration that included BNL, LLNL, SLAC, UCLA – at the Accelerator Test Facility at Brookhaven National Laboratory. A. Tremaine et al.," Characterization of an 800 nm SASE FEL at Saturation", presented at the 2001 Free-Electron Laser Conference, Darmstadt, Germany, Aug. 20-24, 2001.

[52] Such sources were, at the time, envisioned to produce with sub-picosecond pulses of radiation, a time scale incompatible with storage ring generated electron beams.

[53] S.V. Milton, et al., "Exponential Gain and Saturation of a Self-Amplified Spontaneous Emission Free-Electron Laser", Science, Vol. 292, Issue 5524, 2037-2041, June 15, 2001.

[54] V. Sajaev et al., Nucl. Instrum. Methods **A506**, p. 304 (2003) and V. Sajaev and Z. Huang, Nucl. Instrum. Methods, A507, p. 154 (2003)

[55] See "SASE FEL at the TESLA Facility, Phase 2," DESY Report TESLA-FEL 2002-01, June 2002

[56] V. Ayvazyan et al. "Generation of GW Radiation Pulses from a VUV Free-Electron Laser Operating in the Femtosecond Regime," Phys. Rev. Lett., **88**, Num. 10, (2002). Figure 10a and its caption are reproduced from this paper.

[57] Op.cit., DESY32 Figures 10b and 10c are reproduced from this report.

of energy per pulse, E_{rad}, normalized to the average energy per pulse, $< E_{rad} >$, is just what would be expected for a SASE FEL operating the exponential gain regime.

The successes of the FEL experiments at DESY and the excellent agreement between theory and experiment come at the price of enormous care and attention to detail in overcoming major technological challenges in designing and operating an accelerator and beamline system that can furnish a sufficiently high quality electron beam to and through the undulator. Those challenges of realizing SASE FELs include the reliable production of low emittance electron beams, the control of electron energy through the e-beam pulse, the pulse-to-pulse repeatability of the beam characteristics, wakefield effects in the accelerator and in the undulator, beam diagnostics and beam control, etc. Such issues are not peculiar to the SASE architecture but are shared by all short wavelength FELs, though with specifics that differ from project-to-project and that depend on the choice of accelerator technology employed. This review paper will illustrate the specifics of many of these applied physics and engineering considerations in detail in the context of the FERMI FEL design.

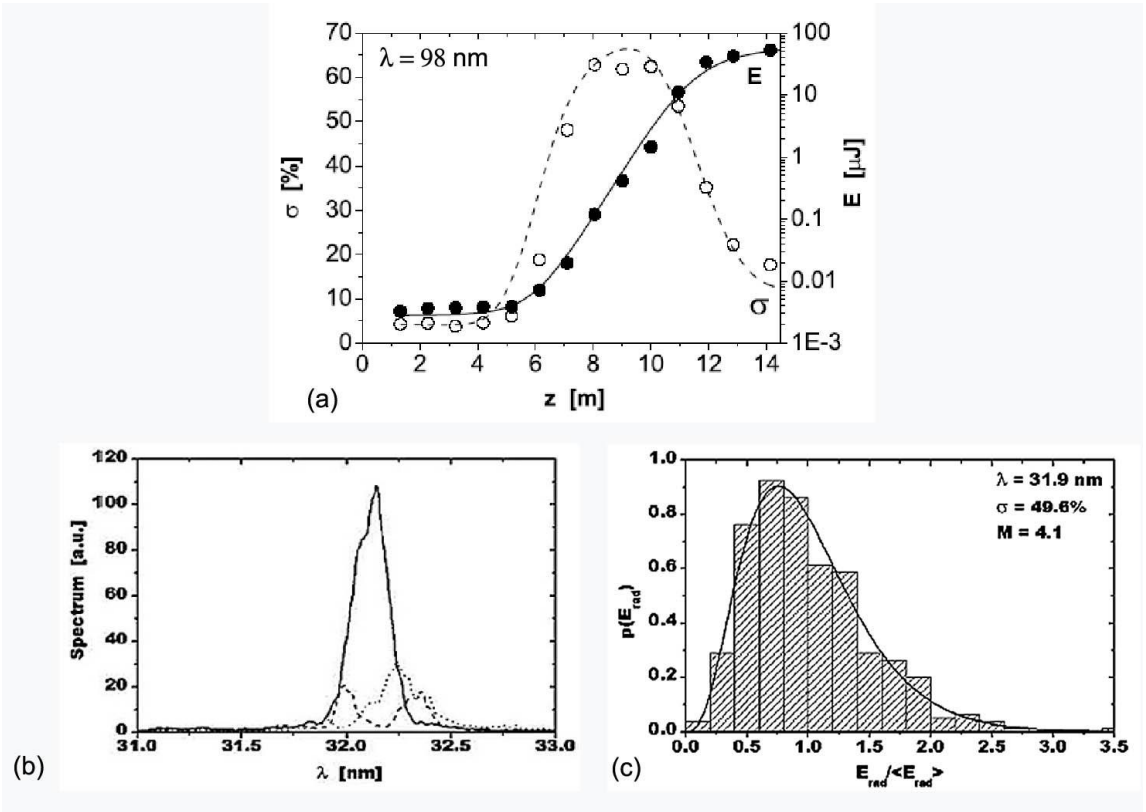

Figure 10 (a) "Average energy in the radiation pulse (solid circles) and the rms energy fluctuations in the radiation pulse (empty circles) as a function of the active undulator length. The wavelength is 98 nm. Circles: experimental results. Curves: numerical simulations with the code FAST." (b) Three single-shot wavelength spectra of FEL radiation pulses measured at the VUV-FEL at 32 nm. (c) Measured probability distribution (histogram) of the energy in FEL pulse energies at 32 nm. The solid curve represents the Gamma distribution $p(E)$ for $M = 4.1$ where M is the total number of optical modes in the pulse. This distribution is the expected one for a high-

gain FEL operating in the exponential gain regime.

III.B.1. ESASE and other modified SASE architectures

In pushing the experience of LEUTL and the TTF FEL to the hard X-ray regime, the XFEL and LCLS designs expose some deficiencies of the simple SASE architecture.

a) Extremely long undulators (>100 m) and great sensitively of FEL output to the delivery extraordinarily bright electron beams to the undulator,

b) Difficulty of synchronizing the FEL signal to ~10 fs as required by the study of ultra-fast dynamics using pump-probe techniques.

c) Lack of temporal coherence of the FEL output

Zholents, et al proposed[58] a technique (current-Enhanced SASE or ESASE for short) to address the first two of these shortcomings. Using the ESASE architecture, they propose to shorten the exponential gain length, making LCLS less sensitive to electron beam emittance. ESASE employs an energy modulator (ultra-short pulse, optical laser plus undulator) followed by a dispersive section to manipulate the electron beam characteristics at high energy, thus shortening the gain length and enabling absolute synchronization of the FEL output with a second laser used in pump-probe experiments.

A related scheme[59] proposed by Saldin et al. foregoes the dispersive section but adds a monochromator at the output of the SASE FEL to selected the wavelength corresponding to the energy modulated portion of the pulse. Without the bunching in the dispersive section the SASE gain length is unchanged. Both approaches derive from the concept[60] of "energy marking" or "laser slicing" a high-energy electron beam via the resonant interaction of a TW laser pulse in a short undulator.

Other proposals[61] to enhance SASE performance also yield the benefit of providing a high precision laser timing pulse for the experimental end stations. Moreover, all these proposals may offer a means of producing sub-femtosecond (~500 as) UV/X-ray pulses.

---

[58] A.A. Zholents, W.M. Fawley, P. Emma, Z. Huang, G. Stupakov, S. Reiche, "Current-Enhanced SASE Using An Optical Laser And Its Application to the LCLS," SLAC-PUB-10713, (2004). Figures 11 is taken from this report. See also Zholents, A.A. and Fawley, W.M., *Phys. Rev. Lett.* **92**, 224801 (2004).

[59] E.L. Saldin, E.A. Schneidmiller, M.V. Yurkov, "Terawatt-scale sub-10-fs laser technology – key to generation of GW-level attosecond pulses in X-ray free electron laser," *Opt. Comm*, **237**, 153 (2004). Hereinafter SSY237.

[60] This concept was first introduced by A. Zholents and M. Zolotorev, "Femtosecond X-ray pulses of synchrotron radiation," Phys. Rev. Lett. 76, 6, 912 (1996). This technique of strong energy modulation was demonstrated experimentally at the Advanced Light Source and used to make 200 fs X-ray pulses. R.W. Schoenlein, S. Chattopadhyay, H. Chong, E. Glover, P. Heimann, C. Shank, A. Zholents, M. Zolotorev et. al , "Generation of femtosecond pulses of synchrotron radiation," Science, March 24, 2000.

[61] P. Emma, K. Bane, M. Cornacchia, Z. Huang, H. Schlarb, G. Stupakov, D. Walz, "Femtosecond and Subfemtosecond X-Ray Pulses from a Self-Amplified Spontaneous-Emission-Based Free-Electron Laser," Phys. Rev. Lett. **92**, (7), 20 February 2004, Pp. 748011-748014. This paper presents a concept of selecting a femtosecond or sub-femtosecond pulse by spoiling the transverse emittance of the electron beam outside of the time slice during which the X-ray generation is desired. The scheme rests on the high degree of sensitivity of the SASE process to the beam emittance.

Presently, however, synchronization at this level is beyond what can be achieved over 200 m to 1 km distances typical of proposed FEL user facilities.

E-SASE on LCLS

In the ESASE architecture a short pulse (30-100 fs) from a high power (1-10 GW), infrared laser (2.2 μm) overlaps a portion of the electron beam at an intermediate energy (4.5 GeV for LCLS) in a short, appropriately tuned undulator (*e.g.* λ_w =30 cm, B_w =1.7 T). The pondermotive force of the laser radiation introduces a periodic energy modulation of the electron beam with relative amplitude 5 to 10 times greater than the uncorrelated energy spread in the beam. Once this laser-marked beam is at full energy, its passage through a bend with sufficient chromatic dispersion transform the energy modulation into a periodic enhancement of the peak current to ~20 kA, significantly reducing the FEL gain length.

Once the electrons enter the long undulator, they emit x-rays via the standard SASE process but with saturation of the modulated portion occurring at roughly half the saturation length of the unaltered portion of the electron pulse. This result is illustrated in Figure 11 for the case of LCLS with the beta function in the undulator optimized for ESASE (12 m). As radiation from the unaltered portions of the electron beam is very far from saturation, the X-ray output from the current-enhanced portions of the beam will be orders of magnitude larger than that from the remainder of the e-beam. The temporal format of the ESASE radiation is a series of uniformly spaced spikes, each of which is temporally coherent.

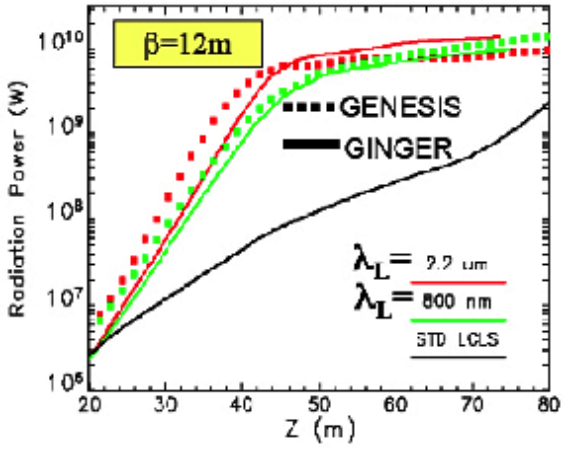

Figure 11. Example of the improvement in gain of the LCLS FEL at 0.15 nm using E-SASE.

Energy-marking in XFEL

The energy-marking approach[62] of Saldin et al. relies on the fact that laser interaction introduces a strong energy chirp within the beam (Figure 12a). When this marked beam passes through the 120 m XFEL undulator, the regions where the energy chirp is largest will have the gain suppressed. This feature can be seen in the calculated result of a typical FEL output pulse such as shown in Figure 12 b. By applying the FEL resonance condition to the curve in Figure 12a, one notes that the temporal structure in panel 10b is

[62] Figure 12a and 12b and their captions are reproduced from SSY237.

correlated to a plot of X-ray energy with time. Therefore, the isolated ultra-short pulse can be extracted from the full FEL output with the use of a monochromator.

A technical difficulty of the energy-marking scheme, is that the monochromator must be designed to survive extremely high power densities at the fundamental and especially at the 3rd harmonic[63] which can be 1% of the fundamental power but which diffracts more slowly. In addition, for pulses shorter than 1fs dispersive effects in the monochromator can easily lengthen the radiation pulse to >1fs. These technical considerations must be addressed before the energy-marking scheme can be considered practical.

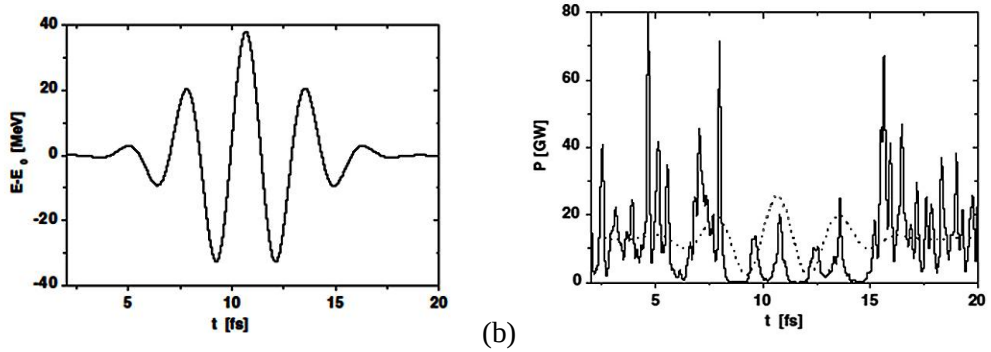

(a) (b)

Figure 12 (a) Energy modulation of the electron beam at the exit of the modulator undulator. The laser parameters are wavelength = 800 nm, W_{peak} = 800 GW, and FWHM pulse duration of 5 fs. (b) Typical single-shot temporal structure of the central part of the radiation pulse. Undulator length is 120 m. Dotted line shows energy modulation of the electron bunch shown in panel (a).

Summary comment

Accompanying the obvious benefits of the enhanced SASE proposals are potentially important shortcomings or uncertainties. It is not known whether potential degradation of electron beam quality from unwanted collective effects such as CSR and wakefields in the accelerator in long undulators will suppress FEL gain. Moreover, both the E-SASE, "energy-marking" and emittance marking schemes waste ~99.8% of the high-energy electrons, implying a marked decrease in average photon flux.

III.C Master-Oscillator Power-Amplifier architectures (MOPA)

III.C.1 Basic principles

A large class of user experiments will require a spectral line width less than □□ An even larger class will require that the FEL system furnish the user end station with timing pulses synchronized to the FEL output to within a fraction of the FEL pulse duration. Both these requirements can be accomplished with a MOPA architecture.[64]

Rather than allowing the FEL instability to grow from shot noise, one can inject an initial radiation signal within the gain-bandwidth of the FEL to co-propagate with the electron beam through the undulator. If the intensity of the injected signal is much larger than the shot noise, the output radiation will approximate (in a manner to be described) the

[63] Z. Huang and K-J. Kim, "Nonlinear harmonic generation of coherent amplification and self-amplified spontaneous emission," Nucl. Inst. and Meth. A **475** (2001) 112–117

[64] As the injected signal need not come directly from an oscillator, this architecture is often referred to as a seeded FEL or in conventional laser parlance, an injection locked amplifier.

temporal coherence properties of the input. In this regard, the free electron laser is different from standard laser amplifiers. In stimulated amplified emission, all the energy from the population inversion is drained into the (narrower) line width of the injected master oscillator pulse. Thus the output spectrum is fixed by the input signal. In contrast, the signal from the FEL grows over the entire gain-bandwidth.

Therefore, when the radiated signal within the line width of the injected signal reaches saturation, amplified shot noise over the remainder of the gain-bandwidth of the FEL creates a large spectral pedestal. If this pedestal must be orders of magnitude smaller than the amplified injected signal, then the intensity of the input signal must exceed the shot noise by orders of magnitude. In the case of the HGHG schemes described in the next section, the input signal power[65] should be at least 10^2 and preferably 10^3 times larger than the shot noise power.

A complication of using a MOPA or injection-locked architecture is that the electron beam energy, which sets the central wavelength of the gain-bandwidth, must be stabilized to well within the gain bandwidth. That is, the energy should be stable on a pulse-to-pulse basis to $\sim\rho/3$. In a simple amplifier system, this limitation could be circumvented by 1) having the input laser pulse longer than the electron beam pulse plus 2) imposing an energy chirp on the electron beam that is greater than the energy jitter of the accelerator. The price that one pays for this circumvention is that a significant portion of the electron beam will be wasted and the possibility of precision timing set by the laser master clock is lost. Finally the MOPA cannot be used directly at wavelengths low which high power laser operation is possible. Instead some process of harmonic up-conversion must be employed.

III.C.2. High Gain Harmonic Generation (HGHG) cascades

That the FEL process generates harmonics of the fundamental frequency in the Fourier components of the electron beam current was recognized early in the development of FEL systems. The first application of this concept as a path toward frequency up-conversion[66] was in the context of the optical klystron[67,68]. Such an experiment[69] was

---

[65] Unfortunately for wavelengths less than 20 nm, laser output signals using harmonic generation in gases are not yet suitable for use as a EUV/X-ray FEL inputs. Progress in this area remains rapid and one can be optimistic about the availability of tunable master oscillators at 20 – 50 nm within the next several years.

[66] See for example, P. Csonka, "Enhancement of synchrotron radiation by beam modulation," Part. Accel., 8, 225 (1978). Also N. A. Vinokwov and A. N. Skrinskii, "Oscillator klystron in the optical band using ultra-relativistic electrons," Preprint INP 77-59, Novosibirsk, U.S.S.R., 1977; A. N. Skrinsky, Novosibirsk, Institute Report INP 78-88. See also B. Kincaid et al., "Free Electron Laser Generation of Extreme UV Radiation," edited by J. Madey and C. Pelligrini, AIP Conference Proceedings No. 118, American Institute of Physics, New York (1983)

[67] N. A. Vinokurov, in Proceedings of the 10th International Conference on Particle Accelerators, Serpukhov, **2**, p. 454. (1977)

[68] The optical klystron is a configuration consisting of two undulators separated by a dispersive section. In low gain systems that typified early FELs, the beam is modulated in energy in the first undulator by an injected laser pulse at the frequency of the FEL resonance. The energy-modulated beam then passes through a dispersive section where the energy modulation is converted into a density modulation. Then beam then passes into the second undulator (the radiator), which is tuned to either the frequency of the injected signal or to an harmonic thereof.

conducted in 1984 using the ACO storage ring as the beam source. The injected frequency of the radiation was 1.06 μm from a Nd:YAG laser. The experiment measured third harmonic radiation (355 nm) from the second undulator at an intensity 100 to 1000 times greater than the spontaneously emitted value.

A fully developed scheme of harmonic multiplication in a multi-stage wiggler was analyzed by Bonifacio and Scharlemann[70] and shortly thereafter extended by Yu[71] to the cascade scheme embodied in the FERMI and BESSY FEL designs The fundamental concept is simple. The FEL process bunches the beam current into thin slabs, roughly one-tenth of an optical wavelength long spaced by an optical wavelength. The Fourier transform of this current distribution contains components (of decreasing magnitude) at all harmonics of the optical frequency. For this reason the FEL output also contains radiation[72] at harmonics of the resonant frequency.

Passage of a beam exiting the FEL through a second undulator tuned to the harmonics leads the beam to radiate coherent spontaneous radiation at that harmonic. If the energy spread in the electron beam is sufficiently small and if the undulator is sufficiently long, the FEL process can amplify the harmonic signal in the second undulator. The first practical realization[73] of this concept to up-convert an initial seed laser pulse was the DUV-FEL experiment conducted by Yu and his collaborators at BNL.

For the DUV-FEL experiment, a 300 pC, 4.5 MeV, 4 ps (FWHM) electron bunch from a 1+1/2 cell photocathode gun with normalized emittance of 3–5 π mm-mrad injected into two S-band SLAC-structures and accelerated to 77 MeV. At this point the bunch was compressed prior to acceleration to the full energy of 172 MeV. The full energy beam was co-injected with a 30 MW, 800 nm seed laser pulse into a modulator (undulator) designed for resonance at 800 nm. Upon exiting the modulator the electron beam entered a dispersive section to enhance the FEL-induced bunching. Finally the beam traversed the radiator tuned to the third harmonic of the injected laser signal.

Figure 13 from the DUV-FEL experiment shows the enormous advantages that the HGHG approach shares will all MOPA realizations of the FEL, namely, the undulator can be considerably shortened and secondly the spectral width is set by the master oscillator (seed laser rather than by the gain-bandwidth of the FEL process). The

---

If the beam current is sufficiently high, the initial radiation could be the shot noise. When placed in a storage ring, the optical klystron could be surrounded by an optical resonator in either an oscillator or regenerative amplifier configuration. As the FEL process heats the beam, such a configuration requires that the synchrotron radiation losses in the remainder of the ring exceed the energy radiated by the FEL or optical klystron.

[69] B. Girard et al., "Optical Frequency Multiplication by an Optical Klystron," Phys. Rev. Lett. **53**, 25, (1984) 2504

[70] R. Bonifacio, L. De Salvo Souza, P. Pierini, E.T. Scharlemann, "Generation of XUV light by resonant frequency tripling in a two-undulator FEL amplifier," Nucl. Inst. and Meth. A: **296** (1-3), pp. 787-790

[71] L. H. Yu, Phys. Rev A **44**, 5178 (1991)

[72] This feature of the FEL has been known from the earliest analyses of the FEL process. Due to interference effects, the radiation from helical undulators does not contain the even harmonics on-axis. Nonetheless the electron beam current does contain Fourier components at the even harmonics.

[73] L. H. Yu et al., Science **289,** 932 (2000) and L.H. Yu et al., "First Ultraviolet High-Gain Harmonic-Generation Free Electron Laser," Physical Review Letters 91 (7), pp. 748011-748014 (2003). Figure 13 and its caption are reproduced from the latter manuscript.

combination of both these considerations mean that the pedestal of radiation outside the signal line width can be exceedingly small, *even without the use of a monochromator*.

The concept of the harmonic cascade is that the radiation output from the radiator can now be used as a high power seed to be injected into a downstream modulator-radiator section. Both the BESSY-FEL and FERMI @ Elettra have produced designs based on the principle of harmonic up-conversion of an injected "seed" signal in a single pass, FEL amplifier employing multiple undulators. The basic principles that underlie this approach to obtaining short wavelength output are:

a) Energy modulation of the electron beam via the resonant interaction with an external laser seed in a first undulator (the "modulator")

b) Passage of the e-beam through a chromatic dispersive section to develop a strong density modulation with large harmonic overtones;

c) Coherent radiation by the micro-bunched beam in a downstream undulator (called "radiator").

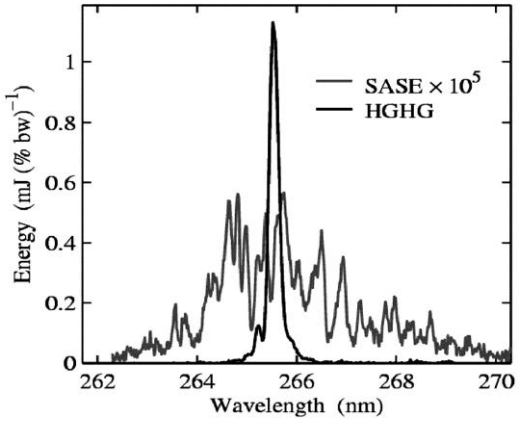

Figure 13. "Single shot HGHG spectrum for 30 MW seed power in the DUV-FEL experiment, exhibiting a 0.1 % FWHM bandwidth. The grey line is the single shot SASE spectrum far from saturation when the 30 MW seed was removed. The SASE spectrum is the background of the HGHG output. The average spacing between spikes is used to estimate the pulse length. The HGHG spectral brightness is 2×10^5 times larger than the SASE undulator is too short to achieve SASE saturation. Were the undulator doubled in length, the SASE would reach saturation, but would have an order of magnitude lower spectral brilliance than the HGHG signal."

An external laser with a beam diameter significantly larger than that of the electron beam provides the initial wavelength-tunable seed signal. This signal, in conjunction with the magnetic field generated by the modulator, produces a strong, transversely uniform, energy modulation $\Delta\gamma$ of the electrons via resonant interaction. The temporal variation of the modulation is ω_0 ($=2\pi c/\lambda_0$, where λ_0 is the seed wavelength). When the length of the modulator is comparable to or shorter than the exponential gain length for FEL radiation power *and* when the number of undulator periods obeys the relation $2N_u\ (\Delta\gamma/\gamma_0) < 1$, the modulator produces insignificant accompanying density modulation (*i.e.*, micro-bunching). The electron beam next passes through a chromatic dispersion section[74] in

[74] The choice of a dispersion section to bunch the beam (rather than continued passage through the undulator) minimizes any phase space distortions of the beam outside the region of temporal overlap with the injected laser pulse.

which path length differences associated with the energy modulation produce a density modulation of the beam. For $\Delta\gamma >> \sigma_\gamma$, (the initial "incoherent" slice energy spread), a strong periodic density modulation is created at wavelength λ_0 containing large higher harmonic components (up to harmonic number $m \sim \Delta\gamma/\sigma_\gamma$).

At this point the electron beam enters the radiator, whose wavelength and magnetic strength are tuned such that the FEL resonance occurs at an integral harmonic *m* of the original seed laser wavelength:

$$l_m = \frac{l_0}{m} = \frac{l_w}{2g^2}\left(1 + a_w^2\right) \tag{23}$$

where a_w is the normalized RMS undulator magnetic strength. For FERMI, the harmonic number, m, varies between 3 and 6 for the first radiator. If this radiator is the final undulator, it is made sufficiently long for the FEL radiation to grow to saturation (or even longer via tapering if greater output power is sought).

For a multistage harmonic cascade, the first radiator is generally made much shorter than that necessary for power saturation. In the so-called "fresh bunch" approach[75] (Figure 14), the duration of the electron bunch is several times longer than the duration of the seed laser pulse. In that case radiation from the first radiator is used to energy-modulate part of the electron beam in a subsequent modulator; therefore, the first radiator is made only long enough that the radiation greatly exceeds the shot noise at λ_R and is sufficient to produce adequate downstream energy modulation. The radiation emitted from the "radiator" is effectively coherent spontaneous emission, the power of which scales as the square of the product of the current and the longitudinal distance inside the undulator (ignoring diffraction and debunching effects).

Following the first radiator is a section (essentially a chicane) that temporally delays the electron-beam in order to make the output radiation temporally coincident with a "fresh" section of the electron beam closer to the beam head. This fresh section of the bunch has not had its incoherent energy spread increased via FEL interaction in the first stage modulator and radiator. Thus, it can be far more easily energy- and density-modulated in the second stage undulators than the "used" electron-beam section that interacted with the seed laser pulse in the first modulator and radiator.

This combination generally leads to a smaller energy modulation at the end of the second modulator. The second stage radiator is usually much longer than that of the first stage both because the initial bunching is normally smaller and because the FEL is normally run to saturation (which requires more distance because the corresponding exponential gain lengths are longer due to the smaller a_w). The process of light emission in the final radiator includes at first quadratic part (as in the first stage and in single-stage FEL-1 configuration) and then an exponential growth regime. Thus it is similar to the classic HGHG scheme of Yu.

[75] Note that the fresh bunch approach demands the energy jitter of the beam significantly less than ρ.

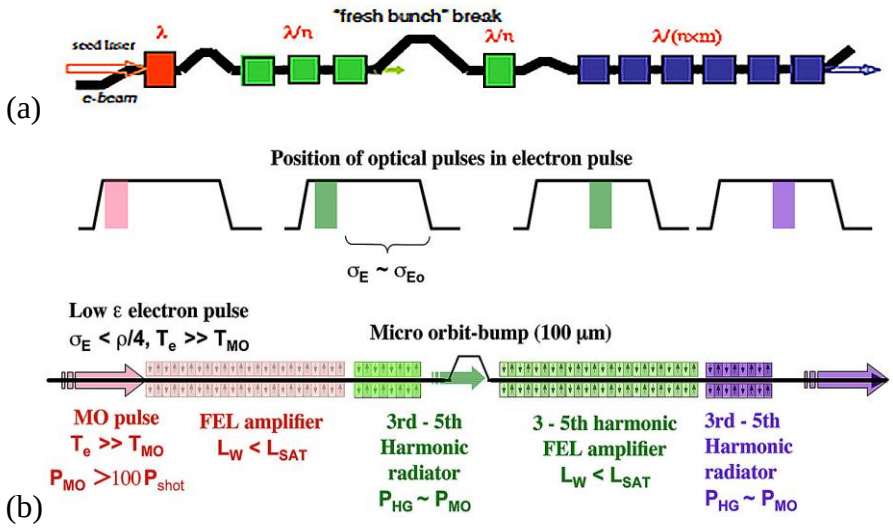

Figure 14. Schematics of (a) the FERMI HGHG cascade; (b) the fresh bunch approach.

The second stage in the fresh bunch approach consists of a modulator, a final radiator, and, in general, an intervening dispersive section. The modulator uses the radiation from the first stage radiator as its seed radiation; it must therefore have its undulator period and magnetic strength tuned to be resonant at that same wavelength. Since the radiation diffracts freely once it departs the first radiator, care must be taken 1) that the temporal delay section is not too long and 2) that the required length of the second modulator does not exceed the Rayleigh range. Otherwise, the coupling between the radiation and the electron beam may be too weak for sufficient energy modulation to develop. The second stage modulator, radiator, and intervening dispersive section are quite similar in concept to the first stage.

In general, the harmonic upshift factor between the second stage modulator and radiator is 4 or less (for FERMI). Moreover, the amount of micro-bunching at the new harmonic in the second radiator is also generally less than half that produced in the first stage because both the undulator parameter a_w and the initial radiation intensity are smaller.

An alternative to the "fresh bunch" scheme in a HGHG cascade is the single-bunch (or whole bunch) scheme, that has been proposed by Brefeld et al.[76] for implementation at DESY (for FLASH) and that has also been studied extensively in the FERMI technical optimization study. In the single-bunch approach, the entire beam is energy modulated by a long laser pulse in the first undulator by an amount smaller than the intrinsic energy spread in the bunch. Nonetheless, after passage through the dispersive section the density modulation at the harmonics exceeds the shot noise at these frequencies. Therefore, in undulator two the FEL radiation signal at the harmonic will have the properties determined by (thorough not identical with) the initial seed laser.

A potential advantage of the single-bunch approach is that the transform limit of the radiation can ideally have a narrower line width than is obtainable in the fresh bunch

[76] W. Brefeld et al., "Study of the frequency multiplication process in a multistage HGHG FEL," Nucl. Inst. and Meth. A **483** (2002) 80–88

scheme. A disadvantage is that the time dependent energy variation within the pulse (chirp) caused by wakefields must be kept flat over a substantially longer pulse.

Brefield at el. also argue that regardless of the particulars of the HGHG, the phase noise on the beam will grow as m^2 where m is the harmonic number of the up-shifted radiation. As a consequence, the noise power, P_n, of each stage of the cascade will grow by the square of the frequency multiplication factor. To obtain a good signal-to-noise ratio in the out put radiation the input laser power, $P_{laser} >> m^2 P_n$ imposing a practical limit on the wavelength that can be reached with a ~200 nm seed laser.

III.C.2.a. Critical design sensitivities for an HGHG user facility

A critical parameter affecting the requisite electron beam duration in an HGHG cascade is the timing jitter of the beam relative to that of the seed laser. In order to assure sufficient overlap between the seed pulse and the electrons, the duration of the electron beam must exceed the sum of the seed pulse duration plus twice the RMS timing jitter. In the case of FERMI, in which the expected RMS timing jitter from the accelerator is ~150 fs, an e-beam pulse duration >600 fs is needed for 100-fs seed pulses. This timing jitter is one of the most demanding requirements on the injector and accelerator subsystems.

Critical to time domain experiments is shot-to-shot repeatability. Ideally, for experiments probing nonlinear (multi-photon) phenomena, shot-to-shot RMS jitter in normalized photon number should be 5% or less. Such a low value seems unlikely with S-band copper accelerators and injectors. The performance is potentially better with a CW superconducting linac in which feed-forward control is possible. Fortunately a large class of experiments can tolerate values as high as 25% by recording the shot-by-shot photon number for post-processing. Other jitter parameters – pointing, virtual waist location and angular divergence jitter, shot-to-shot transverse profile changes – can indirectly affect the intensity on the experimental sample. None of these is likely, on an individual basis, to preclude reaching the goal of 5% (spatially) local intensity fluctuations at the experimental sample; however, taken together they may produce jitter exceeding this goal even in the absence of fluctuations in photon number. Notably, some experiments (*e.g.*, those using gaseous samples) may be insensitive to pointing or profile changes. Finally, the wavelength jitter should be less than the individual shot bandwidth so as not to increase the effective time-averaged, output bandwidth as seen by the user.

Intensity control

While in all FEL architectures scaled to short wavelengths, excessive emittance or incoherent energy spread, σ_E, suppresses gain resulting in low radiated output power, in a multi-stage harmonic cascade, the sensitivity to energy spread is heightened as the nonlinear growth of harmonic micro-bunching leads to a sharp cliff in σ_E beyond which the output radiation in the final stage will be small. Multistage output also displays a sharp cliff for currents much lower than the design current, because the output power from the first stage, being coherent spontaneous radiation, scales quadratically with current. Moreover, if the design of final radiator relies upon strong exponential gain, the output from that stage will be very sensitive to the beam current.

The most sensitive parameter is that of initial electron beam energy. For the MOPA configuration a fractional change of $\rho/3$ (0.1% in the case of FERMI) induces large variations in output power implying stringent shot-to-shot energy jitter requirements. Such a sensitivity to jitter in electron energy is of utmost concern for those time-domain experiments measuring nonlinear (multi-photon) phenomena. Figure 15 displays this sensitivity for FERMI.

The FERMI example is based on a set of calculations done with simultaneous, multi-parameter jitters (seed power, 5%; energy spread, 10%; peak current, 8%, emittance 10%); a set of 400 parameter values were created in which each and every beam parameter was randomly varied following the appropriate Gaussian distribution. The single parameter sensitivity scan (line) shows that energy plays a crucial role in the FEL performance of a seeded HGHG system. The multi-parameter results (dots), remain very well correlated to the electron energy variation, although they show scatter due to the other parameters being varied.

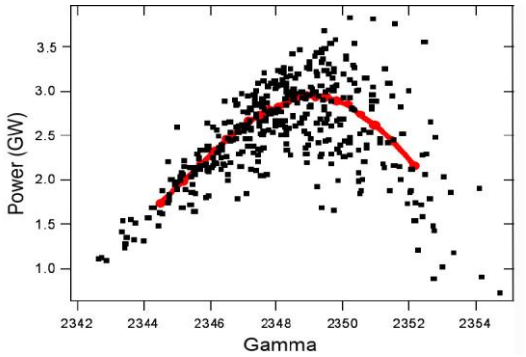

Figure 15. FERMI FEL output power at 40 nm as a function of electron-beam energy in the case of a single parameter only (curve) and multi-parameter (dots) variation.

Spectral control

For frequency domain experiments, shot-to-shot repeatability in photon number is of less concern than preserving central wavelength and the narrow spectral bandwidth of the seed radiation. In an HGHG cascade, the chromatic dispersion sections that produce strong micro-bunching before each radiator also introduce a strong sensitivity of output wavelength to initial energy chirp on the electron beam. In particular, a temporally broad, quadratic chirp in energy leads to a linear chirp in output wavelength making it difficult to reach the transform limit, even when the magnitude of the dispersive matrix element of the transport matrix of the bunching chicanes is made as small as practical. However, this effect is essentially deterministic and does not dilute the longitudinal phase space of the radiation on a microscopic level.

Narrow temporal fluctuations in electron beam energy (such as might develop from the micro-bunching instability) also will broaden the spectral band pass[77] and, if severe enough, actually dilute the microscopic phase space of the radiation. The combination of statistically varying energy chirp on the electron pulse and the use of bunching chicanes also leads to pulse-to-pulse jitter in the central frequency of the FEL that is not seen in

[77] A chirp in the frequency of the injected laser pulse can also broaden the line width.

simple MOPA configurations. This effect is illustrated in the calculations of Figure 16 for the FERMI FEL operating at 40 nm.

For experiments such as resonant inelastic X-ray scattering (RIXS) that probe a small, inelastic scattering cross-section in the presence of a much larger elastic scattering cross-section, the requisite spectral resolution of 10^5 requires that the integrated noise photon level outside the central radiation line width be less than 1 part in 10^5 of the desired signal at the detector. Without spectral filtering using a monochromator, this requirement could be more stressing than that of RMS bandwidth. For example, if the integrated noise power is 1 part in 10^4 but has a bandwidth 100 times greater than the main signal, the total (signal + noise) RMS bandwidth increases by only ~40% from that of the signal, but the unfiltered spectral resolution would still miss the 10^5 criterion by a factor of ten.

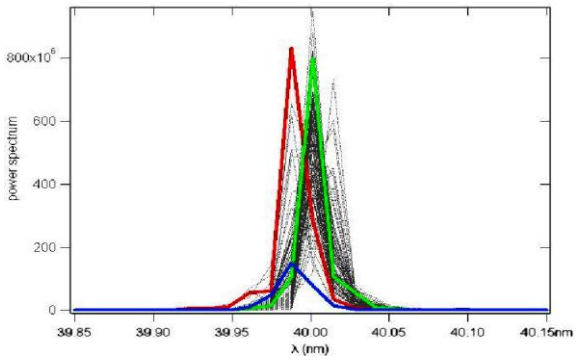

Figure 16. Jitter in the central frequency of the output from the FERMI FEL operating at 40 nm.

III.C.2.b HHG seeded cascades

Presently the limit to which harmonic up-conversion is practical in HGHG arrays is not experimentally established. In the FERMI FELs a design factor of 10 – 15 is contemplated in two stages; the 2.3 GeV BESSY design contemplates a factor of ~200 in four stages. Simulation studies[78] in both projects indicate that the quality of the output radiation decreases as the number of cascade stages increases. An alternative is to replace the first HGHG stage with a gas cell that up-shifts the injected laser pulse via the process of high harmonic generation (HHG).

The HHG process[79] results from focusing a pump laser into a gas to such a power density that the optical field at the interaction point is comparable to the internal atomic field. Ionization tunneling, acceleration, and subsequent recombination of electrons result in bursts of radiation every half cycle of the optical radiation. A sample spectrum of the radiation from Ne is shown in Figure 17[80].

[78] For example see E.L. Saldin, E.A. Schneidmiller, M.V. Yurkov, "Study of a noise degradation of amplification process in a multistage HGHG FEL," (2002) Optics Comm., **202** (1-3), pp. 169-187. The authors conclude that, "The results presented in this paper have demonstrated that the HGHG FEL approach is quite adequate for a 10–100 nm coherent source, but not scalable to an X-ray device."

[79] For a quasi-classical interpretation of the process see P.B. Corkum, Phys. Rev. Lett. **71** (1993) 1994. Also see M. Lewenstein, et al., Phys. Rev. A **49** (1994) 2117.

[80] D. Garzella, T. Hara, B. Carre', P. Salieres, T. Shintake, H. Kitamura, M.E. Couprie, "Using VUV high-order harmonics generated in gas as a seed for single pass FEL," Nucl. Inst. and Meth. A **528** (2004) 502–505

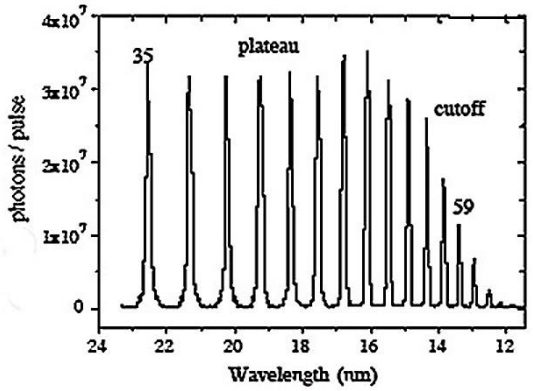

Figure 17. HHG spectrum of Ne from the 35th to 59th harmonic

III.C.3 Hardware tolerances in short wavelength FELs

All short wavelength FELs place tight tolerances on maintaining a precise alignment of the electron trajectory with the central axis of the undulator. In addition to errors in launching the e-beam into the undulator (offset, tilt, and mismatch), other errors are possible within the undulator. These include: 1) tilt and offsets of entire undulator segments, 2) "global" segment mistuning errors such that the average a_w is offset by a constant amount within each segment (e.g. due to an incorrect gap setting), 3) "local" undulator errors due to errors in the strength of individual pole pieces. Local errors can lead both to longitudinal phase errors between the electron beam and the FEL radiation and to the electron beam wandering away from both the central axis of undulator and the radiation.

To lowest order, tilt and offset of the undulator are equivalent to errors (equal and opposite in value) in the initial electron beam position and tilt. In multi-segment undulators, the effect of these errors could, in a statistical sense, grow as $\sqrt{N}$ where N is the number of segments. Hence, if a criterion for beam tilt and offset is a value Y, then the equivalent RMS criterion for the individual segments might need to be reduced to $Y/\sqrt{N}$. However, with active dipole correctors between segments, this estimate may be unduly pessimistic. The technological aspects of alignment tolerances are discussed briefly in section IV.E. 2.

"Global" mistuning of segments leads to an error in longitudinal phase that grows with distance as the beam traverses the undulator. As the phase error approaches $\pi/2$ radians, FEL gain is suppressed. A rough criterion for the RMS accuracy of setting a_w (equivalently the gap opening) in the final radiator can be established by performing a series of computer simulations in which random tuning errors with a given RMS expectation value are applied to each individual radiator segment. An example for FERMI at an output wavelength of 40-nm, is shown in Figure 18. The calculations show that in an average sense, the RMS segment mistuning error in a_w must exceed 0.002 before the output power begins to drop more than a few percent. This constraint appears be relatively easy to meet for the FERMI undulators.

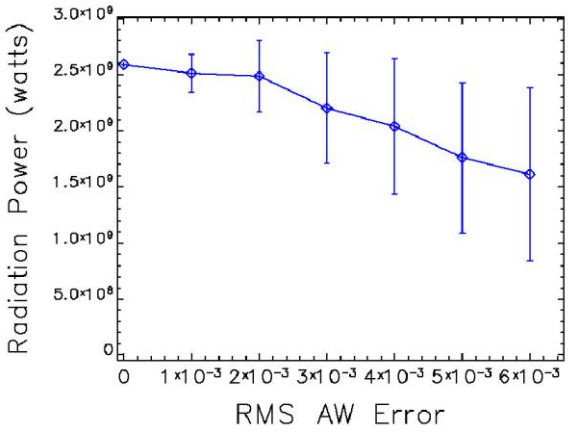

Figure 18. Output radiation power at 40-nm from FEL-1 of FERMI produced by random undulator segment mistuning as a function of RMS error in a_w. The diamond symbol and error bars refer to the mean and standard deviation over 64 independent mistunings. The distribution of errors at individual segments follows a one-dimensional Gaussian.

III.D. Cavity FELs

In an FEL oscillator the undulator is located within an optical cavity resonator as shown in Figure 19[81]. The configuration oscillator requires that electron beam pulses pass through the resonator at a rate set by the round trip time of the photons in the cavity. The multi-MHz rates thus implied naturally suggest the possibility of placing the FEL within a storage ring[82]. In third generation storage rings, a typical peak current per bunch is of order 10 A. For 2 GeV operation, consistent with a FEL operating at 10 nm, and a mean normalized emittance of ~3 π mm-mrad, the gain length would be ~50 m. Therefore a 10 m insertion undulator would have a gain of ~ 1.2. For a resonator with only two mirrors, the mirror reflectivity, R, would have to exceed 0.9 for net gain in the resonator. Unfortunately such high reflectivity is not obtainable at present, but they are sufficiently high[83] to offer an alternative approach to driving the FEL.

In linac driven FELs the limitations on peak current and beam emittance imposed by the storage ring can be avoided. With peak currents raised to ~100 A and emittance improved to ~2 π mm-mrad, the gain length can be reduced by a factor of ten. Thus even in a four mirror resonator, a 10 m undulator can produce an overall gain of 20 –30%. This fact is the basis for the multi-pass, self-seeded Regenerative Amplifier FEL (RAFEL) proposed and tested at infra-red wavelengths by Nguyen et al.[84] at Los Alamos. In the RAFEL the initial signal is not injected but rather grows from noise and is

[81] Adapted from a presentation by H. Padmore, private communication (2006)

[82] This approach has been implemented in Elettra within the EUFELE project, but with a resonance condition limited to an electron energy of about 1 GeV, and a lower limit of the wavelength of about 150 nm, due to the limits in reflectivity of the available materials.

[83] At 11 nm normal incidence reflectivities of ~70% have been measured in a 50 period Mo-Be multi-layer optic, S. Bajt, J. Vac. SciTechnol. 18(2) (2000), pp 557 –559 and P. B. Mirkarimi, S. Bajt, and M. A. Wall, "Mo Si and Mo Be Multilayer Thin Films on Zerodur Substrates for Extreme-Ultraviolet Lithography," Appl. Opt. **39**, 1617-1625 (2000)

[84] D. C. Nguyen, L. M. Earley, N. A. Ebrahim, C. M. Fortgang, J. C. Goldstein, R. F. Harrison, W. A. Reass, J. M. Kinross-Wright, R. L. Sheffield, and S. K. Volz, "Regenerative Amplifier FEL," Proc. XX International Linac Conference, Monterey, California (2000)

amplified by the SASE process. Unlike an oscillator, the RAFEL does not store and build optical energy in the cavity to be switched out after the system reaches saturation. Instead the low-Q optical cavity serves to re-inject a small fraction of the optical power into a high-gain undulator as the seed for the next pass. In the Los Alamos experiment, the low-Q optical cavity was a simple ring resonator consisting of two imaging paraboloids and two annular mirrors that out-couple ~50 % of the generated radiation allowing the RAFEL to come to saturation after few passes through the undulator.

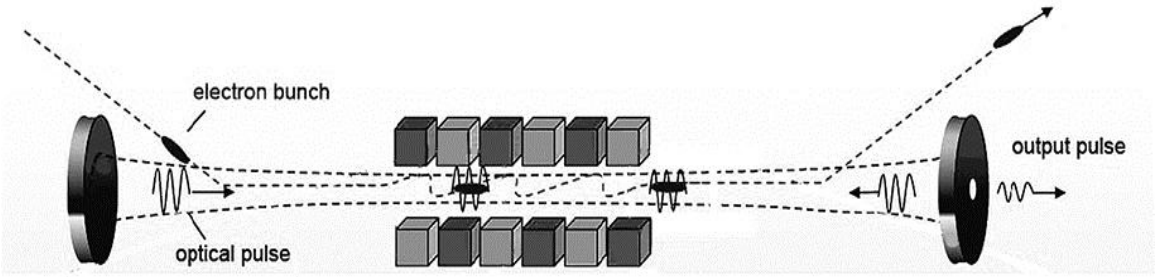

Figure 19. Simplified schematic of a cavity FEL

The RAFEL architecture is ideally suited to be driven by an energy recovery linac and has been adopted for the design[85] of the VUV-FEL (3 – 10 eV) at 4GLS. An advantage of the RAFEL with respect to SASE is that the system smoothes out the shot noise over many passes, thereby considerably reducing the spiky behavior seen in pure SASE FELs. The baseline 4GLS design has three 2.2 m undulator sections yielding a gain of gain ~4 for 300 A operation. At such a high gain the FEL is relatively insensitive to the mirror reflectivity.

Critical issues for this architecture, especially pushing the design into the soft X-ray regime, are appropriate cooling of the mirrors for high average power operation and the damage of the mirrors by FEL radiation at the higher harmonics.

III.E. Attosecond FELs

Zholents and Fawley have proposed[86] an FEL architecture for producing isolated pulses of soft X-rays with a duration of ~100 attoseconds using electrons selected by their previous interaction with an intense, few-cycle, laser pulse. The authors call this process seeded attosecond x-ray radiation (SAXR).'' In principle, SAXR allows excellent temporal synchronization between the attosecond x-ray probe pulse and a pump source that could be the same few-cycle pulse or another laser signal derived from it. Consequently, it is conceivable to track the temporal evolution of atomic or molecular states during a single optical cycle in the process of laser-assisted photo-ionization.

As a specific example they choose 2 nm as the x-ray source wavelength with which to generate 1-nm wavelength, attosecond radiation. As long as an intense, coherent source

[85] N. R. Thompson, M. W. Poole, B. W. J. McNeil, "A VUV-FEL for 4GLS: Design Concept and Simulation Results," Proc. International FEL Conference, Stanford, California, (2005)
[86] Alexander A. Zholents and William M. Fawley , "Proposal for Intense Attosecond Radiation from an X-Ray Free-Electron Laser," Phys. Rev. Lett.., V. 92, Number 22, 4 June 2004. Figures 20 and 21 are reproduced from this manuscript.

is available, attosecond pulse generation at both longer and shorter wavelengths would also be possible with the same scheme.

As illustrated schematically in Figure 20, SAXR requires the combination of an ultra-relativistic electron beam, a few-cycle, intense optical laser pulse and an intense pulse of coherent x-ray radiation, together with a number of magnetic undulators and transport elements. On the left is a source of 100-fs, 100-MW peak power, x-ray pulses. That source could, for example, be an harmonic cascade FEL (HC FEL) configured such that the trailing portion of a sufficiently long (~2 ps) electron bunch is used for the initial x-ray generation. Recall that the fresh-bunch configuration prevents the portion of the beam near the bunch head from having its instantaneous energy spread degraded either by previous FEL interactions in the upstream cascade or even by SASE gain.

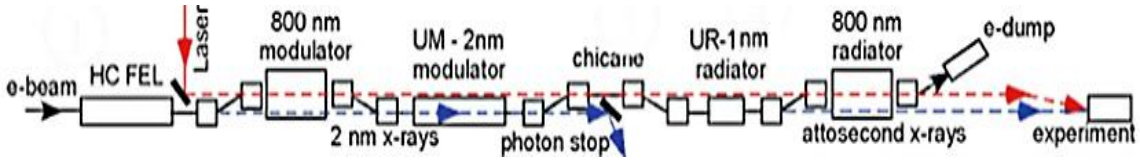

Figure 20. A schematic of the components involved in attosecond x-ray pulse production

An achromatic bend downstream of the HC FEL directs the electron beam into a two-period, undulator magnet (‘‘800-nm modulator’’) where it co-propagates in resonance with an 800-nm wavelength, ~1-mJ, 5-fs laser pulse that temporally overlaps only the undisturbed portion (fresh-bunch) of the beam. The 800-nm modulator imprints a time-dependent electron energy modulation such as shown in Figure 10a. All pulses are tightly synchronized with the original master oscillator pulse of the HC FEL.

A second isochronous bend after the 2-period undulator returns the electrons back to its original axis, while the 800-nm laser pulse continues to propagate along a parallel, offset path. Next, the electrons enter a long undulator modulator (UM) resonant at a 2-nm wavelength. The coherent, 100-fs long, 2-nm output pulse from the HC FEL arrives simultaneously with those electrons that experienced the strong energy modulation at 800 nm and both co-propagate through UM. The undulator parameter a_w of the UM is tuned such that only those electrons very near the peak of the 800-nm energy modulation have the correct energy for resonant FEL interaction with the 2-nm X-rays. As all other electrons fall outside the energy bandwidth of the UM FEL, they are not significantly modulated. By making UM slightly shorter (L_u ~ 5 m) than one full FEL gain length, one assures that there is little SASE action that would produce unwanted micro-bunching at the 2-nm wavelength throughout the entire 2-ps long electron bunch).

Downstream of UM another isochronous chicane enhances the bunching of sub-femtosecond portion of the bunch that has been modulated at 1 nm. The chicane also allows the diversion of the 2 nm X-rays from the attosecond beamline. After passing through the chicane the electrons enter a long radiator resonant at 1 nm. The result, shown in Figure 21, is a multi-GW pulse of 1 nm X-rays with a duration of 110 attoseconds.

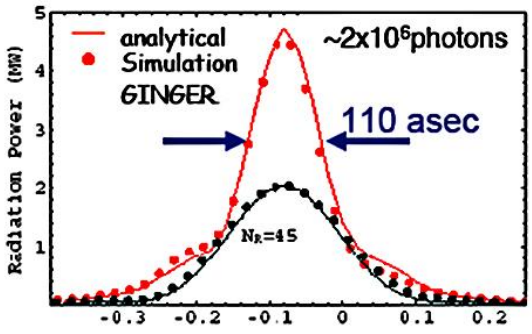

Figure 19. The sub-femtosecond, 1nm output from the Fawley-Zholents architecture

Related schemes of producing sub-femtosecond pulses have been proposed[87] using energy chirped beams. While the authors have claimed the possibility of using optical elements to reduce the pulse duration to 10 attoseconds, no analysis of dispersion in such elements is presented. Given the very large intrinsic bandwidth of such short pulses any beamline would have to be achromatic to at least third order. Moreover the optical elements of such a beam transport would likely need a spatial uniformity at the level of 1 nm to avoid dispersive effects.

III.F. Circumventing limitations on the FEL process

As was discussed in Section III.A.2, excessive energy spread and excessive emittance can severely suppress FEL gain. In 1992 Sessler, Whittum and Yu proposed[88] circumventing these limitations by tailoring the distribution of transverse and longitudinal velocities in the beam. Since that time several investigators have proposed methods including rf-cavities[89], Thompson scattering[90], and laser manipulation[91] to achieve this tailoring (or conditioning) with varying degrees of practicality. The conditioning process involves introducing a correlation between the total electron energy and the transverse random transverse motion of particles.

Emma and Stupakov have cautioned[92] that, in many such schemes, conditioning a nonzero length beam by introducing the correct correlation between betatron amplitude and particle energy leads to betatron mismatches at different longitudinal positions along the bunch that result in an effective increase in the transverse emittance. This difficulty is

[87] E.L. Saldin, E.A. Schneidmiller, and M.V. Yurkov, "Attosecond Pulses from X-Ray FEL with an Energy-Chirped Electron Beam and a Tapered Undulator," Proceedings of FEL 2006, BESSY, Berlin, Germany

[88] A.M. Sessler, D. H. Whittum, and L.-H. Yu, Phys. Rev. Lett. **68**, 309 (1992).

[89] N.A. Vinokurov, "Multisegment undulators for short wavelength FEL," Nucl. Inst. and Meth., **375**, Pp 264-268, (1996)

[90] C.B. Schroeder, E. Esarey, W. P. Leemans, W.P., "Electron-beam conditioning by Thomson scattering," Physical Review Letters **93** (19), pp. 194801-1-194801-4

[91] A.A. Zholents, "Laser assisted electron beam conditioning for free electron lasers," Phys. Rev. ST Accel. Beams **8**, 050701 (2005). Figures 23 and 24 are reproduced from this manuscript.

[92] P. Emma and G. Stupakov, Phys. Rev. ST Accel. Beams **6**, 030701 (2002).

avoidable[93], but it does constrain the acceptable conditioning processes. Assuming that practical difficulties can be overcome, one could realize benefits as dramatic as displayed in Figure 22 for a soft X-ray FEL (2.5 GeV, 0.5 kA) operating at 1 nm.

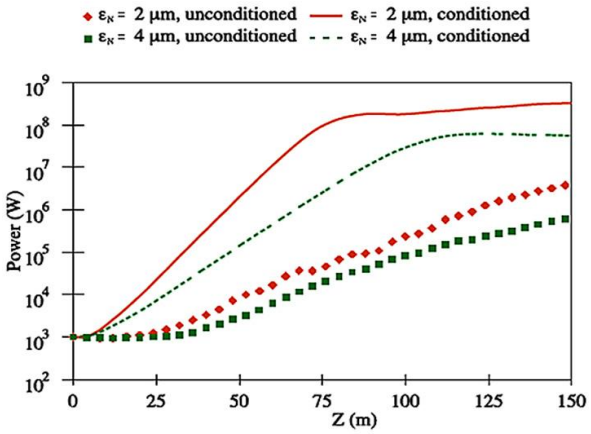

Figure 22. Effect of emittance conditioning on the radiation power as a function of undulator length in a 1nm FEL. The calculations assume that all electrons in the beam are conditioned.

The laser-conditioning scheme proposed by Zholents (Figure 23) extends the rf-conditioning approach concept introduced by Vinokurov to optical wavelengths. It displays a further, practical limitation on conditioning proposals, i.e., introducing proper correlations in some of the beam comes at the expense of spoiling the effective emittance of other portions (Figure 24). In the Zholents-Vinokurov schemes only half the electrons are properly conditioned; the remainder of the beam suffers an increase in the spread of transverse velocity resulting in little gain for these portions. The optical scheme has a second practical difficulty: timing in the beam-laser interaction in the second undulator must be controlled to a small fraction of an optical wavelength.

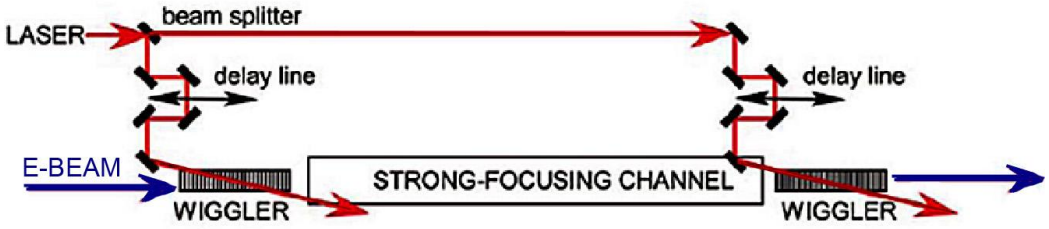

Figure 23. The laser conditioning scheme of Zholents is derived from the Vinokurov scheme.

While experiments have been proposed to demonstrate the predicted benefits of beam conditioning, this exciting prospect awaits a definitive test.

[93] A.Wolski, G. Penn, A. Sessler, and J.Wurtele, "Beam conditioning for free electron lasers: Consequences and methods," Phys. Rev. ST Accel. Beams, **7**, 080701 (2004). Figure 22 is reproduced from their manuscript.

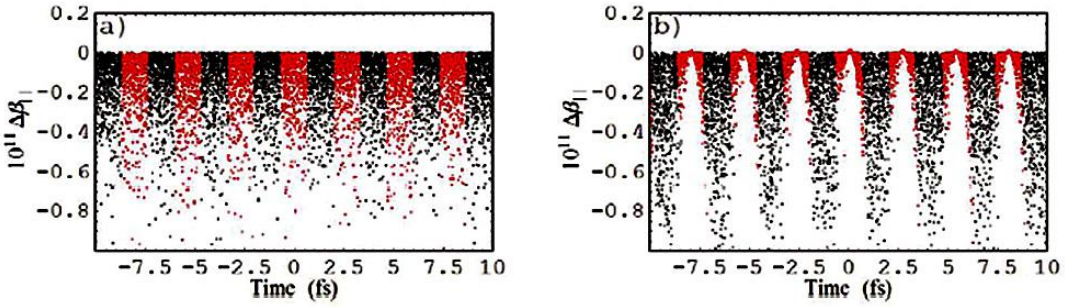

Figure 24. A distribution of the electron longitudinal velocities ($10^{11}\beta$) for unconditioned (a) and conditioned (b) electron beams. The uncorrelated energy spread of the particles is ignored.